NASA Contractor Report 182176

Preliminary Design Study of Hydrogen and Ammonia Resistojets for Prime and Auxiliary Thrusters

Russell J. Page, Willis A. Stoner,
and Larry Barker

R. J. Page Company
Santa Ana, California

October 1988

Prepared for
Lewis Research Center
Under Contract NAS3-23337

National Aeronautics and
Space Administration

CONTENTS

SUMMARY

The designs of two hybrid resistojets, one of a thrust level of 667 mN (150 mlb_f) for primary propulsion, and one of 44.4 mN (10 mlb_f) for auxiliary control for use with either hydrogen or ammonia are described. The design techniques used to forecast the temperature distributions using mathematical modeling by a personal microcomputer are outlined. BASIC language is used throughout to give the designer rapid interaction and control in debugging using the interpretive mode. A compiler is added to reduce the run times of parametric design studies.

For both designs integrating a compact first stage coiled heater, a relatively high voltage device, with a concentric tubular gas heater offers direct matching of the 28 V terminal of the spacecraft system. For primary propulsion the maximum heater wall temperature needed may be kept to less than 55°C over that of the required gas temperature at the throat for hydrogen or ammonia by use of the concentric tubular final stage.

The analysis of the 667 mN primary resistojet, at a gas temperature of 2500°K, chamber pressure of 3.16 atmospheres for hydrogen or ammonia separately, gives the following performance. The specific impulses are 828 and 406 seconds with electric powers of 3.09 and 1.98 kW, respectively. The heater efficiency on a total power basis is .96 and .94, giving overall total power efficiencies of .81 and .66.

The use of recently developed grain stabilized rhenium with refractory metal oxides is employed for all high temperature elements to significantly enhance their endurance strength. High purity alumina is used for insulator seals in the required areas.

The small size and increased life demanded of the auxiliary thruster compared to the primary thruster require a more robust hybrid heater. A bicoil is used to achieve the required resistance and heat transfer required than would be from the scale down in size from the primary thruster. The bicoil mesh is formed by two concentric coils of opposite rotation to form a sturdy self supporting structure without insulators. The wire intersection points are spot welded to provide adequate rigidity.

The analysis of the 44.4 mN auxiliary resistojet at a gas temperature of 2500°K and a chamber pressure of 3.16 atmospheres for hydrogen or ammonia, results in specific impulse of 757 and 375 seconds with electric powers of 244 and 162 watts, respectively. The heater efficiency is found to be lower on a total power basis than the primary design at .88 and 83. This results in overall total power efficiencies of .60 and .47.

INTRODUCTION

Studies of large manned space stations (circa 1969) for NASA showed that high performance resistojets have important applications to attitude and orbit control (refs. 1 and 2). Both specifically chosen high performance gases and biowaste gases available as propellants were studied. These studies showed that not only lower propellant consumption over the long life resulted, but there were other important advantages. These were minimizing contamination of the spacecraft environment, limiting noise, vibration, etc. In order to deliver the high performance required to be competitive in these studies, these resistojets, unlike the much earlier units, required: 1) higher temperatures than early flight resistojets of the 1960 period; 2) reliable operation for long periods of time (years); and 3) high energy efficiency, that is, low thermal losses and high conversion efficiencies to jet energy resulting in thrust.

The present report is a formal summary of informal specific design studies of resistojets using high performance gases, H_2 or NH_3, performed for Lewis Research Center and delivered in the 1982-1983 period for internal use when studies for a current manned space station were again evolving. By informal reporting procedures including technical conferences, details of the design calculations, drawings, fabrication procedures, material choices, etc., were submitted. The basis for the designs presented here were evolutions of the concentric tubular type resistojet developed and evaluated in 8,000 hour life tests in support of the early NASA space station studies (refs. 3, 4 and 5) in the .044 Newton class and, subsequently, further developments (refs. 6, 7, 8 and 9) in the .667 Newton size. A new hybrid feature is introduced to the thrusters for matching its terminal voltage directly to the spacecraft main power voltage, assumed to be 28 Vdc.

A program written in the BASIC language was used for mathematically modeling the temperature fields, heat fluxes, electric current and voltages, and gas dynamics resulting from the design perturbations tried. The program was run on a personal microcomputer of as low as 128K RAM capability. Finally, it takes the opportunity to update the materials used.

The latest 667 mN (150 mlb_f) concentric tubular design, (ref. 7) built (ref. 8) and experimentally evaluated (ref. 9) operated at a terminal voltage of 14.7 volts and 208 amperes for an applied electrical power of 3051 watts. Freedom to independently adjust the terminal voltage so as to match spacecraft power would reduce the power matching (weight) problem substantially. Further, the simultaneous reduction in current would reduce the spacecraft power conductor size. However, early attempts to increase this voltage by reducing the wall thickness

of the ohmically heated concentric shells or increasing the number of such tubes was reported (ref. 6) to not be feasible for such a design. The contribution of the current design is a hybrid feature to be described, which is a first stage heat exchanger in series, both electrically and gas dynamically, with the concentric tubular design. It consists of a multicoil type exchanger. This type design has the classical high wire overtemperature characteristic compared to resulting gas temperature. This is not a serious problem in this design in that its temperature range is low. It works well within long-life criteria at the lower temperatures, yet the coil allows adjustment of the overall voltage readily to 28 volts when connected in series with the concentric tubular stage. The second stage concentric tubular design can be made to have the gas finally approach very closely to the maximum wall temperature, a feature favorable to high performance.

The problem of designing for 28 volts at the terminals in a 44 mN thruster is significantly more difficult than in the 667 mN size. A different kind of additional stage in addition to the first stage coil, a bicoil, is required.

Analytical and experimental studies of viscous and transition flow nozzles are required before such designs can be made with great confidence. This was beyond the scope of this effort and is an area for future study. However the nozzle efficiencies used in the projected performance are attainable, and have been realized before (refs. 6 and 11).

The resistojet is simple in concept. There are basically two sections: 1) an electric gas heater, and 2) a gas accelerator or thrust producer (nozzle). The first is primarily a heat transfer problem. The second is supersonic - laminar to transition flow field problem involving miniature nozzles.

In order to address the major thermal impact of the addition of the first stage heater, the mathematical model herein described was developed. While the notion of thermal modeling to determine the temperature field is an old one, the one presented here in light of modern personal computers allows the design engineer to begin to obtain results from his adjustments to the design. Reference 10 describes a subsequently developed, more generalized approach to the problem by the same authors. It is considerably more rapid and general than that reported here.

DESIGN OBJECTIVES

Two resistojets were designed. One is for primary propulsion and the other for auxiliary. Both were to serve as laboratory models usable for research on hybrid propulsion concepts. This included the ability to disassemble the units following a test. At the same time, flight weight design philosophy was to be used as far as feasible. The resistojets were to be operable on either hydrogen or ammonia. Performance goals for both thrusters with either propellant are shown in table I. The independent design variables include a thrust of 667 mN (150 mlb_f) for the primary thruster, and 44 mN (10 mlb_f) for the auxiliary. Both units are designed for a gas temperature of 2500°K, and a chamber pressure of 3 atmospheres. An important goal was that they be operable on 28 volts with hydrogen and at least 22 volts on ammonia.

While operation at 28 volts is clearly desirable, the difficulty of achieving this in the smaller auxiliary thruster designs was recognized. A trade off between thruster design difficulties and the alternate requirement for power adaptation should be examined. the primary thruster had a minimum design life goal of 2000 hours with the capability of withstanding 400 interruptions of electrical power; while, for the auxiliary thruster, a goal of 8000 hours with 4000 cycles was set.

Numerous considerations enter into the selection of materials for a resistojet. Properties of interest include: electrical resistivity, ductility after high temperature operation, low and high temperature strength, weldability, and formability to name but a few. Since life requirements are high, the design task tends to focus on achieving the required life while maintaining reasonable cost and weight figures.

The concentric tubular type resistojet was first introduced in 1962. Because of early experimental work, criteria for estimating the life of this type of unit are fairly well known (ref. 3). The materials used for construction, besides serving their functions, require resistance to the long term effects of high temperatures. Life governing factors are sublimation of heater surfaces, redeposition of vaporized material on cooler critical areas, endurance stress rupture, creep elongation, cyclic fatigue, chemical attack of expellants on walls and insulators, and metallurgical instabilities.

An attractive design is one which works each element equally based on its limiting criteria. To do this, the designer must have accurate data on the endurance of the materials used; and have a suitable method for forecasting temperatures, stresses, etc., in critical parts. One goal of this program was to develop a rapid mathematical computational model to determine

TABLE I

RESISTOJET DESIGN PERFORMANCE OBJECTIVES

	Primary Propulsion		Auxiliary Thruster	
Propellant	H_2	NH_3	H_2	NH_3
Thrust, mN	667	667	44.4	44.4
Gas temperature, °K	2500	2500	2500	2500
Chamber pressure, atm	3	3	3	3
Specific impulse, sec	828	406	757	375
Expellant flow, g sec^{-1}	8.219×10^{-2}	1.675×10^{-1}	5.992×10^{-3}	1.210×10^{-2}
Electric power, W	3093	1984	244.5	164.7
Total power, W	3438	2083	269.7	171.7
Terminal voltage, V	28	22.4	TBD	TBD
Current, A	110.5	88.5	TBD	TBD
Throat diameter, mm	1.339	1.339	0.348	0.348
Divergent section area ratio	Optimum	Optimum	Optimum	Optimum
Total power efficiencies				
Overall, η_o	0.788	0.637	0.612	0.476
Heater, η_H	0.976	0.960	0.910	0.840
Nozzle, η_N	0.807	0.663	0.673	0.567

effects of thruster design changes on temperature distribution heat fluxes and fluid flows in advance of testing.

The design effort for both thrusters was directed at the following areas:

1) Improving and simplifying the space power system to resistojet matching by increasing the resistojet's design terminal voltage to that of the system;

2) Improving the thruster performance by increasing the exit gas total temperature to as close to the heater maximum wall temperature limit as possible;

3) Identification of recommended materials and processes;

4) Documenting the basis for the design selected by means of detailed drawings, materials specifications, fabrication processes, and assembly procedures.

THERMAL ANALYSIS PROCEDURE

The overall performance evaluation parameters used here are defined in Appendix A. The mathematical thermal modeling of both thrusters are based upon specific, explicit node diagrams constructed for each case as are shown as figures 14 and 15 of Appendix B. A description of the heat balance program is given. Both the general outline of the program and details of the calculation methods are described there for the two thrusters. The reader is referred there for details.

A later, more generalized, method is described in reference 10 where the model basis for the thermal analysis is a generalized system of orthogonal elements in cylindrical coordinates. This model can quickly be shaped to fit an axisymmetric problem. The relationships between elements are activated with references set to material resource data banks to use. The initial time saved is significantly reduced by this later method.

PART I - DESIGN OF A RESISTOJET FOR PRIME PROPULSION

Description of the Configuration

The hybrid resistojet concept is described in figure 1 with the radial scale exaggerated for clarity. There are three gas heating zones in series, the regenerator, the coiled wire heater, and the classical concentric tubular heater. The coiled wire heater and the concentric tubular heater are separately powered for laboratory flexibility. In a flight design these would be internally connected. The design contains two vacuum jackets, one each between the three heaters, to reduce gaseous thermal conductivity losses radially. To prevent high thermal stresses, an expansion compensator is designed so as to permit the inner sections to axially expand relative to that of the case without building severe stresses. Both fibrous and radiation shields are used, the locations of electric insulators are noted.

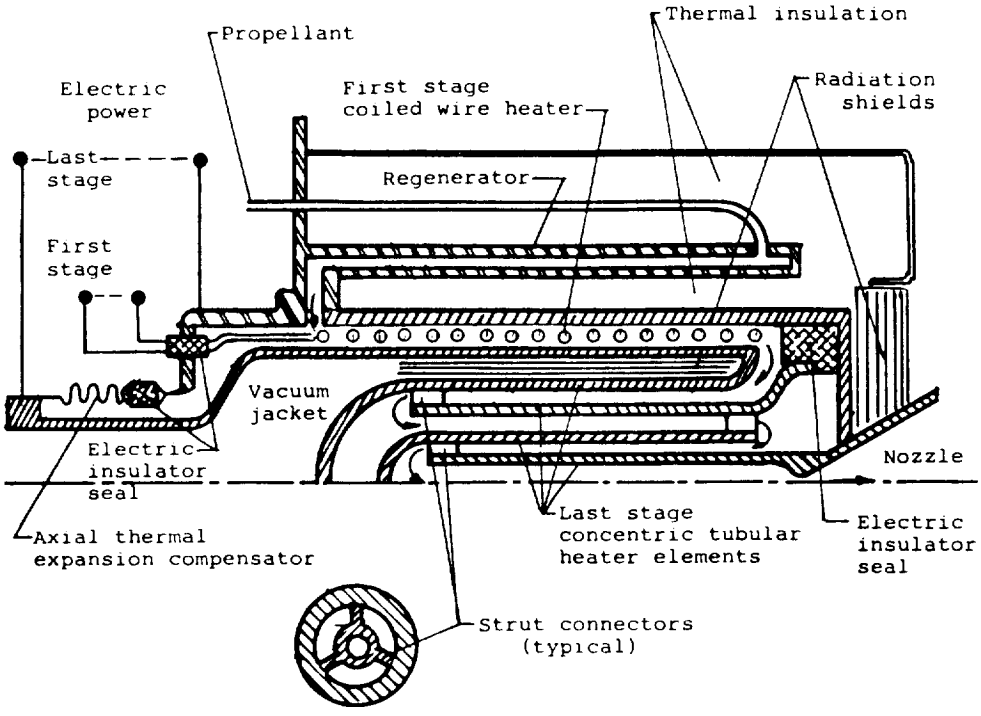

Figure 1.- Hybrid resistojet concept for prime propulsion.

The resultant geometry of the hybrid 667 mN (150 mlb$_f$) resistojet is shown to scale in figure 2. The callouts of the components are identified in table II. This is the final configuration resulting from the study. The basis for selecting the specific geometry is described herein.

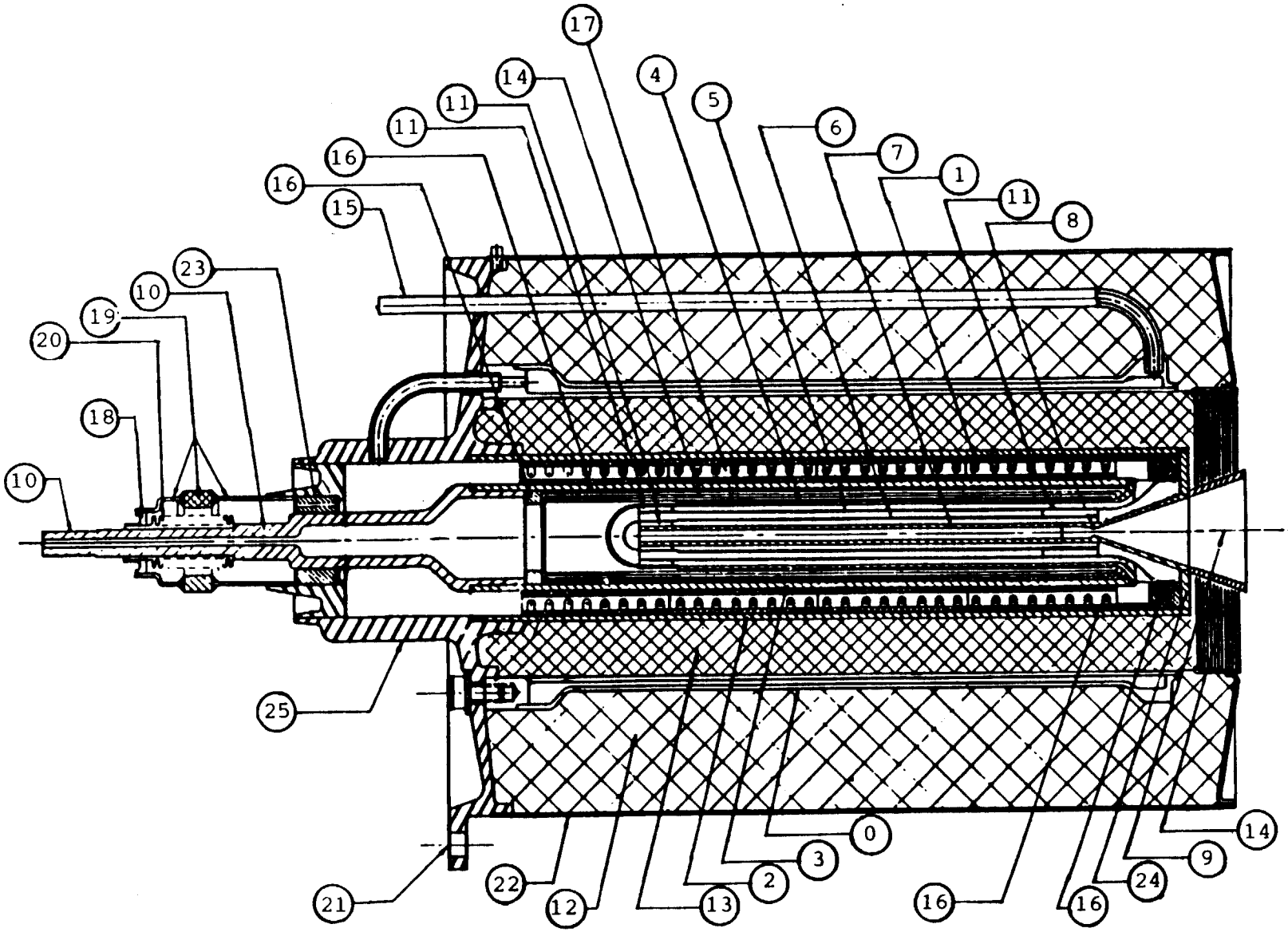

Figure 2.- Preliminary design assembly of the 667 mN (150 mlb_f) resistojet for prime propulsion.

TABLE II
COMPONENTS OF THE 667 mN (150 mlb$_f$) RESISTOJET

No.	Description	Material
0.	Thermal regenerator	CRESS
1.	Hybrid coiled heater-exchanger	*GSRe/Al_2O_3
2.	Outer pressure case	GSRe
3.	Inner pressure case	GSRe
4.	Entrance concentric tubular heater pressure vessel (domed end)	GSRe
5.	Second concentric tubular heater (funnel end)	GSRe
6.	Third concentric tubular heater (domed end)	GSRe
7.	Final concentric tubular heater	GSRe
8.	Nozzle throat and initial expansion	GSRe
9.	Nozzle - final expansion	GSRe
10.	Inner case stem and power terminal	Mo
11.	Radial struts - electric conductor	GSRe
12.	Thermal insulation - low temperature	Al_2O_3 (fibrous)
13.	Thermal insulation - high temperature	ZrO_2 (fibrous)
14.	Thermal radiation shields	GSRe
15.	Propellant inlet line	CRESS
16.	Electric insulators	Al_2O_3
17.	Coiled heater support	Al_2O_3
18.	Adapter ring	CRESS
19.	Ceramic electric insulator - seal	Al_2O_3
20.	Expansion compensation bellows	CRESS
21.	Thruster mounting pad site	CRESS
22.	Insulation canister assembly	CRESS
23.	Electric insulator - bearing	BN
24.	Outer case end	GSRe
25.	End mount	CRESS

* GSRe is grain stabilized rhenium (Ref. 12)

Gas heater.- Physically the hybrid gas heater component is divided into three zones, each thermally separated radially from the others by an effective vacuum Dewar and other insulations. In earlier resistojets (ref. 3), with thrust of 44 mN (10 mlb$_f$), this technique was shown to be a most effective means of insulation. A significantly lower gas thermal conductivity is created by lowering the Knudsen No. to a number much less than 1. This involves the use of low gas pressure and small characteristic lengths. It replaces the continuum regime where thermal conductivity is independent of gas pressure with the molecular regime and is where thermal conductivity is proportional to pressure thus controllable.

Two such evacuated regions are used. The first is between the regenerator (0) and the first powered stage, coiled heater exchanger (1). It is filled with fibrous insulation and exposed to space vacuum. The second is between the coiled heat exchanger and the outer concentric tube exchanger (4). It uses radiation shields (14) to reduce the radial radiation term, and is vented to space vacuum by means of the inner case stem (10).

Regenerator: This is the first gas pass. It is located between the inner (13) and outer (12) insulation surrounding the heater. The gas is heated regeneratively in this pass recovering most of the heat that would otherwise have been lost through the insulation. Contrary to earlier designs, the gas feed tube enters at the nozzle end and flows back toward the mount of the thruster. This arrangement had been avoided previously to keep the higher temperatures away from the mounting flange which tends to have a high thermal loss. However, it was found by means of the mathematically computationally modeling of the heater that the axial distortion of temperature in the heater itself is substantially reduced if the first electrically heated pass (in this case the second pass, the hybrid coil heater (1)) flows toward the nozzle. As a result, the present hybrid design has an estimated gas temperature at the nozzle throat that is only 55°C below the maximum wall temperature. This compares with more than 110°C in earlier designs, as analyzed here and confirmed experimentally in reference 9. The heat loss could be minimized by thermally isolating the mounting flange. A further refinement that could be included later would involve the use of two regenerative passes. The first pass would flow toward the nozzle after effectively cooling the housing, while the second pass would correspond to the one used in the present geometry but entering the annulus internally.

Hybrid coiled heater: This is the second gas pass. It lies in an annular passage between two heretofore relatively heavy tubes (2 and 3) that served as an earlier regenerative pass and pressure vessel (ref. 7). The thickness here has been reduced in half from earlier designs. Although these walls conduct current, their resistance is low and the electric heating in the walls is small. Rhenium wire coils are provided in his pass only. They supply most of the gas heating. Alumina guides and liners are used to assure that the coils do not touch each other or the walls resulting in an electric short. The use of the high temperature electric insulator, alumina, determines the maximum value of the wire temperature that may be used. It is limited to 2140°K which leads to a design with no coils used after the second pass.

By sizing the coil wire correctly, it is possible to find a design with the heater coil and the nested tubes connected in series operating at 28 volts overall. This can be done without going to excessively thin wires. In the present design, the wire diameter was taken as fixed 1.3 mm (.051 inches). For the laboratory model, this stage was elected to be powered separately for diagnostic reasons. Table III summarizes the first stage heater.

TABLE III
FIRST STAGE HEATER COIL
PHYSICAL DIMENSIONS

Heater wire diameter, mm	1.3
Number of parallel circuits	3
Coils per circuit	2
Total heater wire length, each circuit, mm	880
No. of turns per coil	5.77
Coil assembly wire spacing to wire diameter ratio	2.5
Pitch diameter of coils, mm	23.5
Resistance, Ω	0.1818

An alternate design for the heater coil involves packing the coiled wire tightly in alumina powder which is encapsulated in a molybdenum tube. Only the spacing mandrel would be required. No electric insulation in the first electrically heated gas passage would be required, allowing more flow and room for the encapsulation of the coil. The latter might be a more satisfactory design in that the inevitable diffusion of rhenium over the surfaces of the coiled heater support (17) might cause ultimate shorting.

Concentric tubular heater: Gas passes 3, 4 and 5 are annular passages between conventional nested tubes. The thin tube walls, which are of rhenium, serve as resistance heaters, and provide for some additional heating of the gas. This stage is described in reference 7. The purpose of the nested tubes is to increase the gas temperature above that obtainable with the coil heater which is limited by the need for electrical insulators. The merit of the concentric design is that the maximum gas temperature asymptotically approaches closely that of the wall producing a high gas temperature. For this reason, it is the final stage. The large number of tubes provides the electrical resistance required for this stage without using tube walls as thin as would otherwise be required.

In the sixth and final pass (7), the gas flows through a circular tube which connects directly to the nozzle (8). This pass is characterized by, a) high thermal conductive losses at the nozzle end which cool the wall, b) low convective heat transfer between the wall and the gas, and c) low resistive heating in the relatively thick walled center tube. These characteristics are considered fortuitous. The reduced nozzle temperature helps to reduce thermal losses, particularly nozzle radiation losses, while the low convective heat transfer permits the exit gas temperature to be nearly as high as the maximum wall value attained. The maximum wall temperature naturally tends to be at the center of the resistojet as shown later.

The thruster is thermally insulated by a layer of fibrous zirconia insulation (13) surrounded by a layer of fibrous alumina insulation (12). Most heat losses through this are recaptured by the thermal regenerative assembly. The balance passes outward to the (22) insulation canister assembly, hence, thermally to the environment through radiation, gas conduction and metal conduction.

Note that thermal radiation shielding (14) is shown around the nozzle extension. The thermal radiation shield is made in two sectors so as to fit around the nozzle extension prior to installation of the insulation and its retaining insulation canister assembly (22).

Nozzle.- No computational gas dynamical analysis of the nozzle resulting in its performance efficiency was undertaken. The nozzle chosen for use here was that of the earlier 3kW resistojet (ref. 6). The nozzle efficiency, η_n reported there was measured to be 88%. The chamber pressure of 3.16 atmospheres chosen here as compared to the 8.8 of reference 6 could be expected to have somewhat lower performance. The goal values chosen for the study can be expected. The nozzle is defined by table IV.

TABLE IV
NOZZLE DESCRIPTION FOR 667 mN DESIGN

Configuration	Conical
Half angle, α	17.8°
Area ratio	212
Throat (geo.), mm	1.339±.005

Electric system.- The two exchanger stages for the laboratory unit have separate terminals. This is done so as to diagnostically evaluate each system separately and be able to vary the final design power ratios between the first and last stage heaters for both hydrogen and ammonia with but one experimental coil.

The electric description of the coiled wire for the baseline first stage heater-exchanger chosen is shown in figure 3 and Table III The heater is formed as a set of six wire coils each with a pitch diameter of 23.5 mm, of 5.77 turns, with an overall axial length of 110 mm. The six coils are wound, forming a six lead screw (nested coils) about the same axis as the thruster. Electrically three parallel circuits are used consisting of two coils in series per circuit. Each of the six coils begins and terminates at 60° circumferentially from its neighboring coil. The two coils in each circuit are connected together at the nozzle end and to the respective 28 and 7.7 volt busses at the mount end.

The electric current path for the concentric tubular circuit is as follows. From the electric connection which includes a thermal dam (ref. 7) at the mount (21), the current flows forward through the outer case (2) to the outer case end (24), hence to the nozzle (8) and through the inner heating element (7). The current leaves the inner heating element, through the struts (11) to the next element (6) as is made clear by the figure. It then passes through the struts (11) and the second element (5). The path continues through its struts and the heater tube (4) and, hence, along the inner case and the inner case stem (10) to the rear power terminal.

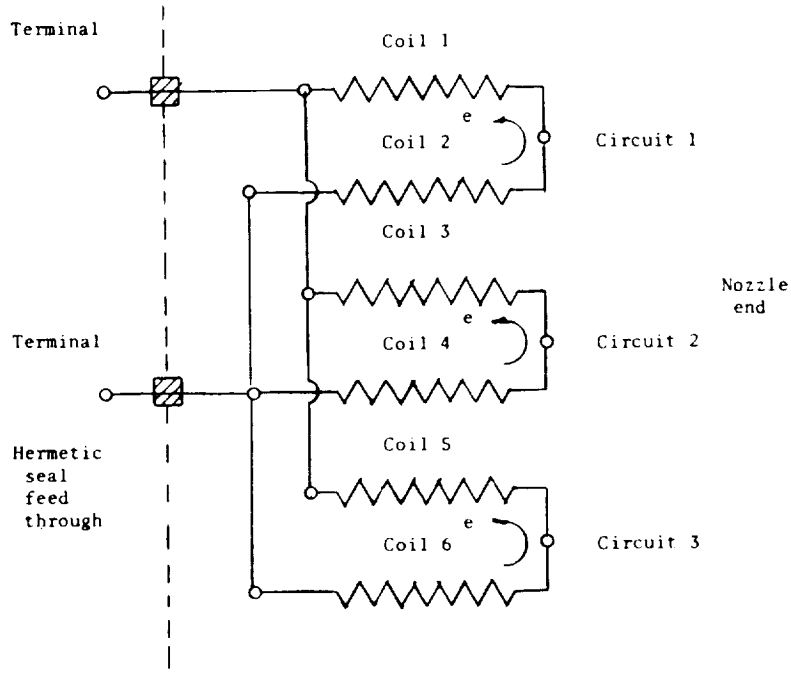

Figure 3.- Electric schematic of first stage heater.

Mechanical system.- The inner assembly is centered in the mounting flange by a boron nitride insulator bearing (23) through which the stem (10) passes. The inner assembly is attached to the outer assembly by a stainless steel bellows (20) which maintains a pressure integrity, but permits differential thermal expansion. The bellows is attached to one end of a metallized ceramic hermetic seal (19). The other end of this composite part is attached to the mount (21) to complete the pressure envelope. The basis of this type design is given in reference 3.

Materials.- From the studies to date, rhenium remains the outstanding heating element material. Any further improvement would be in the area of stabilizing its grain size to protect the geometric shapes of the sophisticated parts and their strength during the long high temperature operation required (ref. 12).

A new electric insulator is proposed and has been used in the design. This is high purity alumina. It can be expected to be useful in such service to temperatures of at least 2150°K.

Results and Discussion of the Analysis

Results of the analysis presented in plots of the temperatures are shown in Figures 4, 5 and 6. Energy distribution diagrams are given in Figures 7a and 7b.

Temperatures.- One purpose of the analysis is to indicate and control locations where the temperature may become excessive. It is important that the amount that the maximum wall temperatures exceeds the exit gas temperature be kept as small as possible. Some temperature difference is necessary to drive the convective heat transfer. The results show a maximum wall temperature of 2550°K occurred at the entrance to the inner tubular heater for the case with a hydrogen gas stagnation temperature of 2500°K at the throat. Some cooling of the gas occurs because the nozzle and the downstream end of the tube are cooled by radiation from the nozzle surface. Since the gas is cooled slightly in the region approaching the nozzle, it must first be heated to a temperature higher than the required exit value. Temperatures in this region are summarized in table V for the two propellants.

TABLE V
CRITICAL TEMPERATURES
MAXIMUM WALL AND GAS AT THROAT

Temperature	Hydrogen	Ammonia
Maximum wall	2550	2555
Maximum gas	2529	2523
Gas at the throat	2500	2500

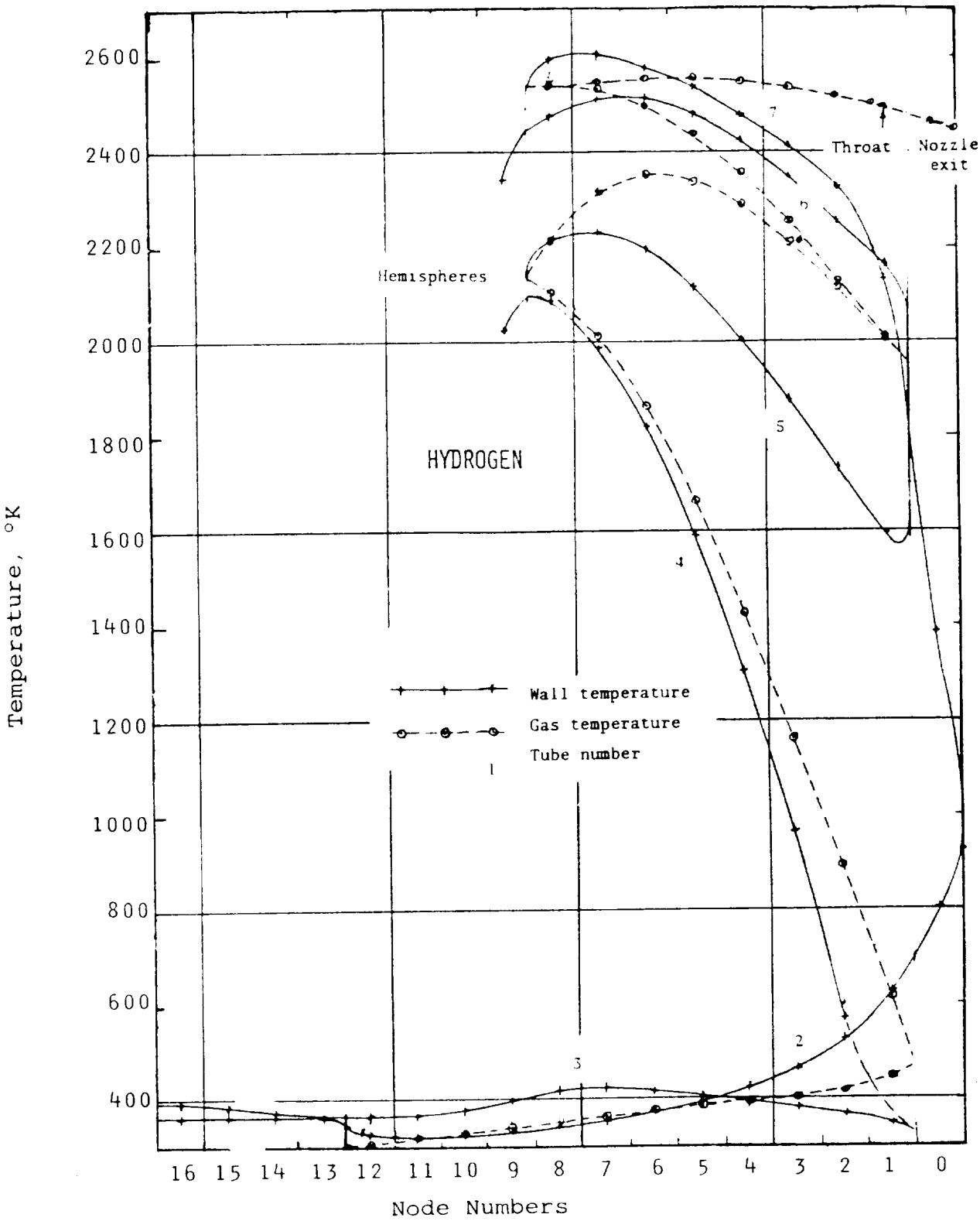

Figure 4.- Temperature distribution, operating on hydrogen, of the concentric tubular resistojet design of reference 7 from the thermal modeling analysis.

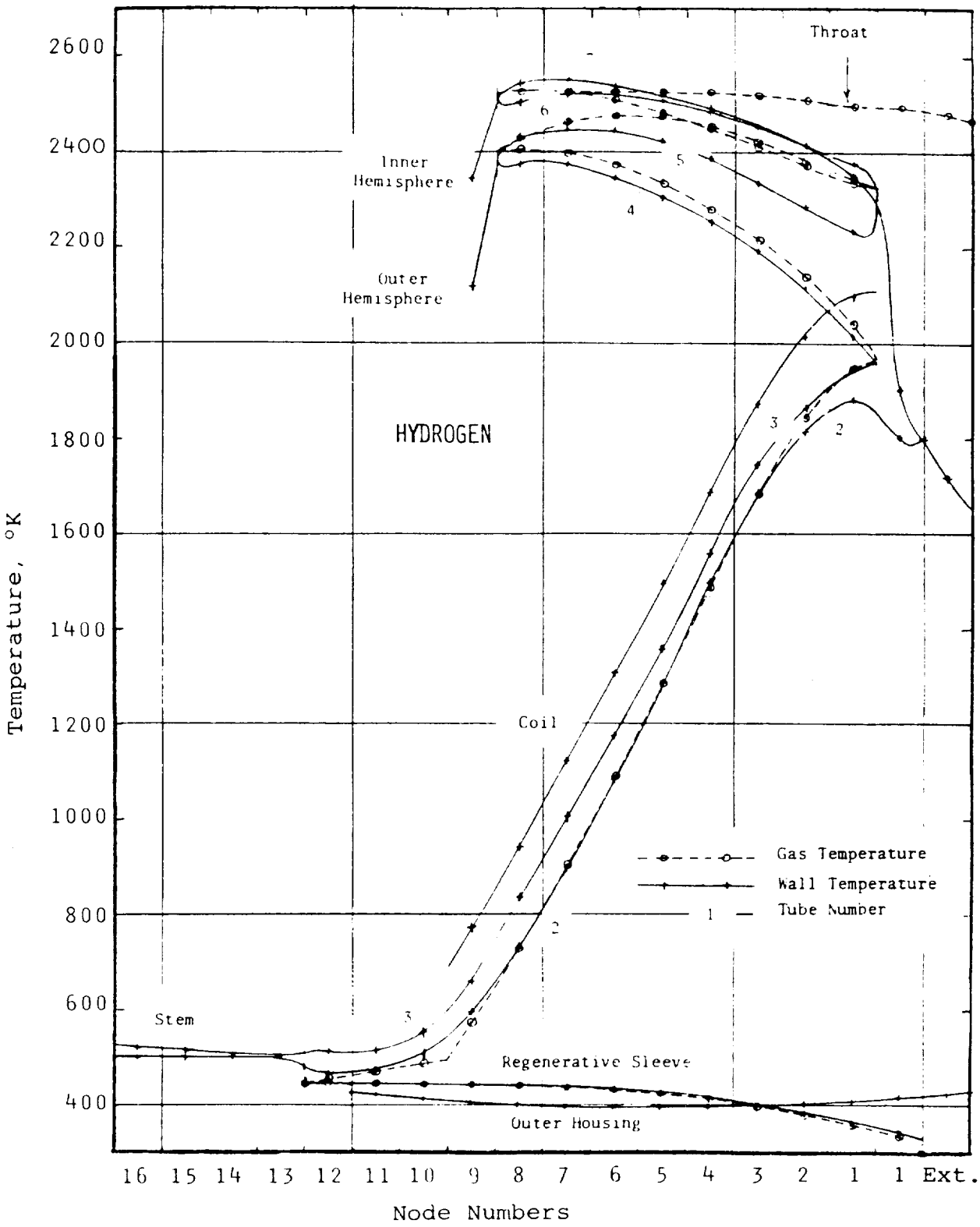

Figure 5.- Temperature distribution of the 667 mN hybrid concentric tubular resistojet operating on hydrogen from the thermal modeling analysis.

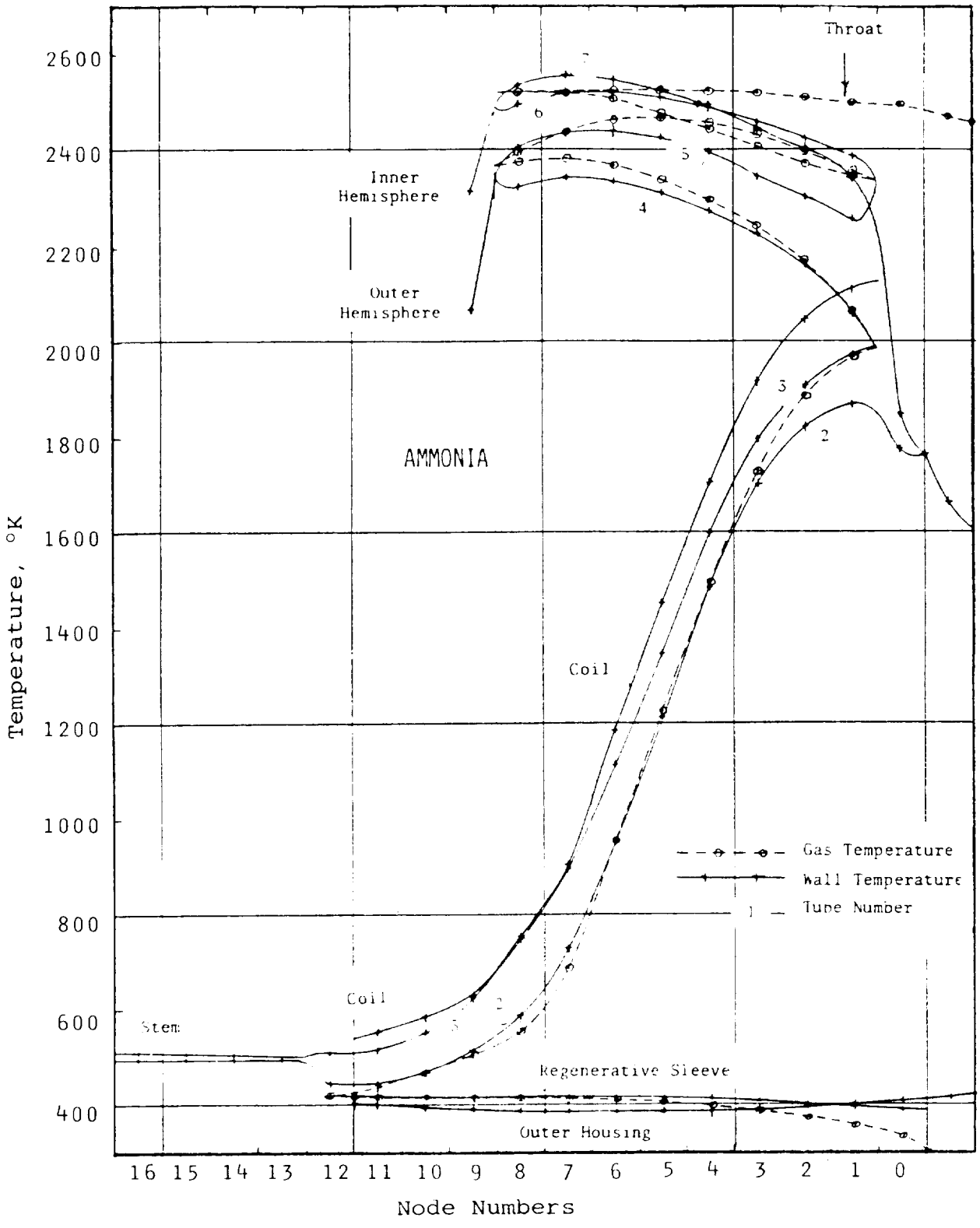

Figure 6.- Temperature distribution of the 667 mN hybrid concentric tubular resistojet operating on ammonia from the thermal modeling analysis.

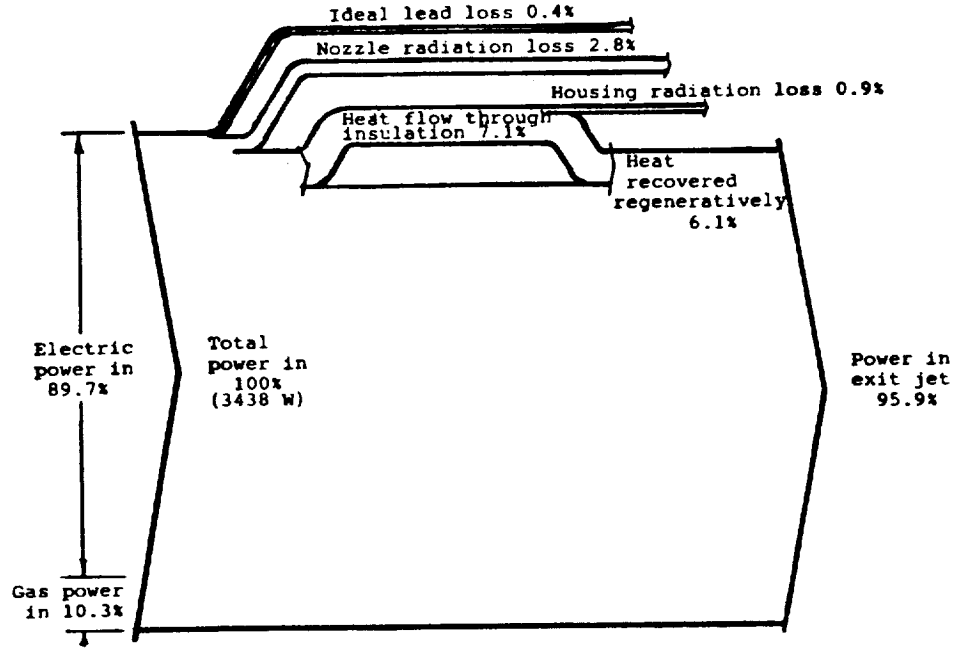

a) Hydrogen

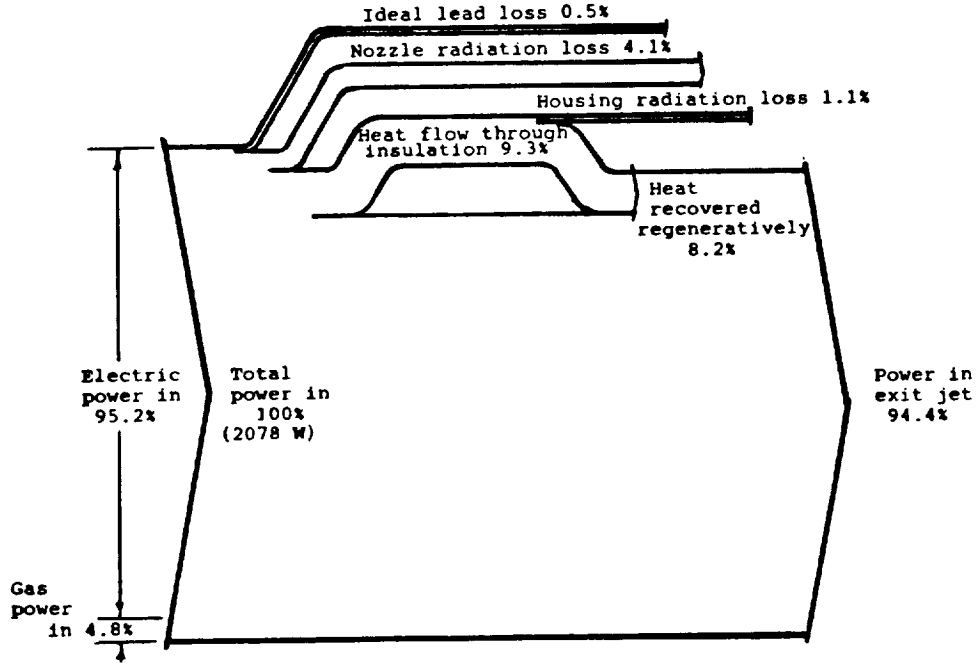

b) Ammonia

Figure 7.- Estimated steady state energy distribution of the 667 mN hybrid concentric tubular resistojet at total gas conditions of temperature of 2500°K and pressure of 3.16 atmospheres at the throat.

This amount of over-temperature is considered acceptable. It is considerably less than was experienced in earlier designs. Two features of the present design keep the over-temperature low:

1) Gas flows toward the nozzle in the first electrically heated passage. This passage has the wire coil heater and increases the gas temperature rapidly to about 2000°K, unlike its earlier design (ref. 7). This keeps the temperature at the nozzle end of outer case (2) high and markedly reduces cooling of the nozzle (ref. 7) by heat conducted through the outer case end (24) and across the gas passages. Compare Figure 4 with Figure 5 to see this temperature distribution difference.

2) The circular inner tubular heater (7) passage used in the last pass connecting to the nozzle has less surface area and is not as effective as the other passes as a convective heat transfer surface. This allows the tube wall near the nozzle to be cooler than the gas without seriously reducing the exit gas temperature.

Although any reduction in gas temperature reduces the specific impulse attainable, there is no disadvantage to allowing the nozzle to run cooler. In the present design, most of the surface of the nozzle is several hundred degrees cooler than the gas temperature at the throat. This reduces the heat loss due to radiation from the nozzle surface to ambient. If all of the nozzle surface was held at 2500°K, the radiation loss given by the program would be 382.7 watts compared to an actual 95.61 watts with hydrogen and 84.07 watts with ammonia. Since tradeoffs are involved, a detailed study of nozzle losses is needed to assist in the choice of suitable nozzle designs and suitable wall temperatures in the nozzle region.

Losses.- Although thermal radiation from the nozzle was found to be the most important loss mechanism in the present thruster design (being three or four percent of the input power), we are not yet in a position to recommend design changes to alleviate this condition. This is because the radiation loss is largely dependent on the nozzle design. If we disregard other effects for the moment, this loss can be reduced by:

1) Reducing the nozzle area ratio;

2) Increasing the inlet gas pressure combined with a reduction in nozzle exit area;

3) Increasing the nozzle divergence angle to reduce the radiation "cavity" effect;

4) Reducing the nozzle wall temperature;

5) Choosing a surface material with lower emissivity.

A trade-off can be expected between radiation loss and other forms of nozzle loss such as viscous ones. The design choice should depend on a more detailed study.

An indication of the importance of the cavity effect was obtained by running the program with the nozzle wall temperature set at a uniform 2500°K. At this condition, computational analysis gives a radiation loss of 382.7 watts. The emissivity for the rhenium wall is .328. The corresponding figure for a simple disk of rhenium equal in size to the nozzle exit area is 217 watts, so the cavity effect (like a hohlraum) corresponds to an apparent emissivity that is 76 percent higher.

Although the present design is not rigorously optimized, it illustrates the feasibility of reducing housing losses to something in the neighborhood of one percent using good insulation and a regenerative cooling passage. At this low level the loss effect is within the objectives of this design. The added weight is the only compromise in performance.

It was expected that the losses with ammonia would be higher, on a percentage basis, than those with hydrogen. The two cases were run with the same throat diameter, the same gas pressure and the same gas temperature at the nozzle. Under these conditions, the electric power input with ammonia is about 65 percent of the value with hydrogen. If the losses were unchanged, they would be more than half again as large on a percentage basis. However, the program showed loss percentages that are only slightly higher than those shown for hydrogen. This results from the assumption that the gas closely approaches the equilibrium condition as it dissociates. On this basis, nearly half of the ammonia would dissociate in the regenerative cooling passage. The result is more effective cooling, less loss through the housing, and some reduction in radiation loss from the nozzle. The residence time for ammonia in the regnerative passage is estimated to be about 200 milliseconds. A calculation of the extent to which equilibrium conditions would be approached has not been attempted.

The computer program did not include an estimate of losses in the electrical leads; or, in its final form, losses by conduction through the mounting structure. Instead, an idealized lead loss has been calculated manually, and the assumption has been made that the mounting structure can be combined with the electrical leads so that the calculated loss accounts for both functions. It has been shown that the lead loss is minimized when the leads are sized so that there is no net thermal conduction (where they attach to the hot terminal on the engine). See reference 3 for the thermal dam design concept. With the relatively high operating voltage and moderate terminal temperatures in the present design, it was found that the minimum lead loss could be held to something like one-half of one percent. This

suggests that the lead loss can be kept small in a practical design.

Calculated losses are illustrated in diagram form in Figures 7a and b. The overall thermal efficiency including lead losses of gas heater and nozzle is estimated to be 95.9 percent with hydrogen and 94.4 percent with ammonia. The calculations were carried out and presented with a degree of precision that is hardly justified by the accuracy of assumptions used in the calculation of heat flows. This was done to facilitate the examination of the effects of small design changes on performance.

Gas dynamics.- The Reynolds numbers in both gas heater and nozzle indicate the laminar regime everywhere. For the coiled heater stage from inlet to outlet, the Reynolds numbers based upon flow channel diameter were 185 to 70 and 270 to 86 for hydrogen and ammonia, respectively. For the concentric tubular heater typical Reynolds numbers were 1300 and 1650 for hydrogen and ammonia, respectively. At the nozzle throat the Reyolds numbers for hydrogen and ammonia were 2040 and 2600, respectively. The Mach number varied from about .003 at inlet to the first stage to .25 at the exit just before the nozzle.

Power supply requirements.- Although an effort was made to size the heating elements to simulate a case with the wire coil and the nested tubes operating in series, the program was actually run with two elements on separate circuits so that temperatures at the coil exit and at the nozzle could be controlled separately. This was a requirement for the initial laboratory engine to provide greater operating flexibility. The heat balance shown in table VIa gives the following operating conditions (omitting lead losses).

TABLE VI
POWER SUPPLY REQUIREMENTS -
WIRE COILS AND NESTED TUBES

a) Initial Results for Independently Powered Stages

Propellant	Element	Voltage (V)	Current (A)	Power (W)	Resistance (Ω)
Hydrogen	Coil	19.03	102.3	1946	.1860
	Concentric	9.59	117.3	1125	.0818
	System			3070	
Ammonia	Coil	14.52	87.9	1276	.1652
	Concentric	7.51	92.2	693	.0815
	System			1969	

Since the two stages must operate electrically in series, their design currents must be the same. The resistance of each stage is adjusted uniformly to give the same i^2R as before. This requires a minor adjustment in wire diameter and tube thickness which has no effect on the validity of the thermal analysis. TABLE VIb summarizes series operation.

TABLE VI (Continued)
b) Adjusted Characteristic for System (Series) Operation

Propellant	Element	Voltage (V)	Current (A)	Power (W)	Resistance (Ω)
Hydrogen	Coil	17.74	109.7	1945	.1620
	Concentric	10.26	109.7	1125	.0935
	System	28.00	109.7	3070	.2555
Ammonia	Coil	14.26	89.5	1276	.1593
	Concentric	7.74	89.5	693	.0865
	System	22.00	89.5	1969	.2458

Estimated performance.- The estimated performance presented in Part I is summarized in table VII.

TABLE VII
ESTIMATED PERFORMANCE FOR PRIMARY PROPULSION

Propellant	H_2	NH_3
Thrust, mN	667	667
Gas temperature, °K	2500	2500
Chamber pressure, atm	3.16	3.16
Specific impulse, sec	828	406
Expellant flow, mg sec^{-1}	82.2	167.5
Electric power, W	3085	1978
Total power, W	3438	2078
Terminal voltage, V	28	22
Total power efficiencies		
Overall, η_o	0.774	0.626
Heater, η_H	0.959	0.944
Nozzle, η_N	0.807	0.663

PART II - DESIGN OF A RESISTOJET FOR AUXILIARY PROPULSION

The Problem of Scaling Down

A resistojet designed for 44.4 mN (10 mlb_f) of thrust is significantly smaller than the 667 mN (150 mlb_f) size considered in Part I. If it were feasible to simply scale down the Part I design, all dimensions would be reduced by a factor of about 3.87. However, a number of difficulties would arise if this were attempted.

1) The requirement for a long life for the auxiliary thrusters 8000 hours versus 2000 for the primary, generally places a lower limit on the heating element thickness; which, for the auxiliary thruster, is incompatible with the scaled down dimensions.

2) It would be desirable to operate the resistojet directly connected to a standard 28 volt power supply. A high operating voltage decreases the lead losses as well as avoiding power conditioning losses.

It can be shown that, although direct scaling of a heating element to smaller size increases the resistance, the increase is not enough to maintain the same operating voltage. It is clear that a new type of heater coil geometry is needed to provide the necessary life, while avoiding the losses and the added weight associated with low voltage and the use of power conditioning equipment.

3) As the size of a resistojet is reduced, the thermal losses due to conduction become an increased fraction of the total power. This is because the temperature gradient in the insulation (and in other conductive heat flow paths) increases as the size is reduced. Even with careful design, it appears to be necessary to accept lower efficiencies in the ten millipound size range.

Description of the Configuration

The key features of the final configuration are shown in figure 8 and table VIII. The detailed design features such as metal to ceramic seals mounting pads are not shown in figure 8, but are similar to those of figure 2, the 667 mN thruster. It is significantly smaller than its predecessor which is described in reference 3. Figure 9 shows these two units in profile outline for comparison purposes. The reduction in size is largely attributable to the use of coil type heating elements to augment the heating action of the concentric tubes. Particularly in small size engines, the total tube length becomes excessive if the full 28 volts is required across the concentric tubular heaters alone.

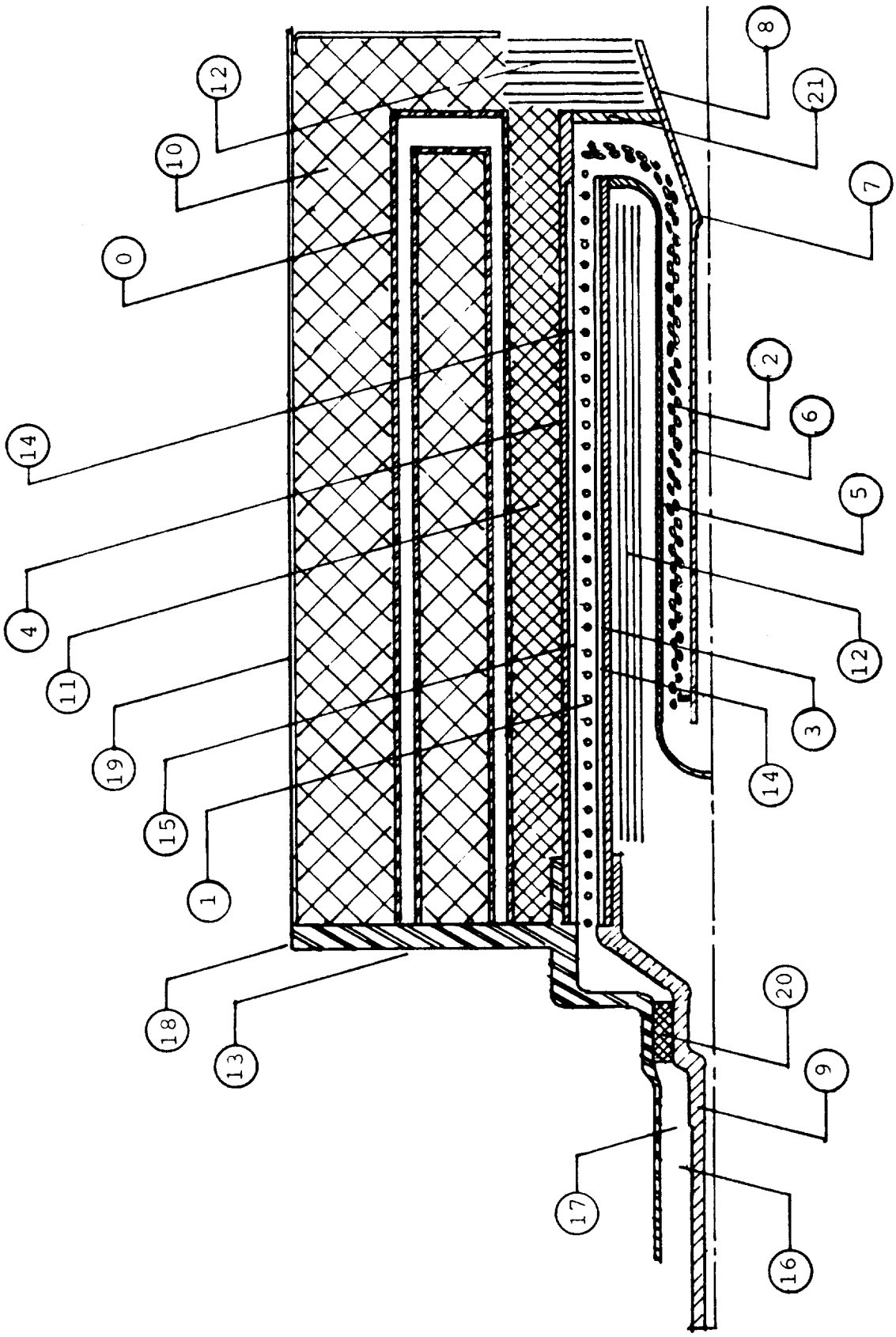

Figure 8.- Preliminary layout of hybrid 44.4 mN (10 mlb_f) resistojet for auxiliary propulsion.

TABLE VIII

COMPONENTS OF THE 44.4 mN (10 MLB_f) AUXILIARY RESISTOJET

No.	Description	Material
0.	Thermal regenerator	CRESS
1.	Entrance coiled heater exchanger	GSRe/Al_2O_3
2.	Bicoil heater-exchanger	GSRe
3.	Inner pressure case	GSRe
4.	Outer pressure case	GSRe
5.	Entrance concentric tubular heater (domed end)	GSRe
6.	Final concentric tubular heater	GSRe
7.	Nozzle throat and initial expansion	GSRe
8.	Nozzle - final expansion	GSRe
9.	Inner case stem	Mo
10.	Thermal insulation - low temperature	Al_2O_3 (fibrous)
11.	Thermal insulation - high temperature	ZrO_2 (fibrous)
12.	Thermal radiation shields	GSRe
13.	Propellant inlet line	CRESS
14.	Electric insulators	Al_2O_3
15.	Coiled heater support	Al_2O_3
16.	Ceramic electric insulator - seal site	Al_2O_3
17.	Expansion compensation bellows site	CRESS
18.	Thruster mounting pad site	CRESS
19.	Insulation canister assembly	CRESS
20.	Electric insulator - bearing	BN
21.	Outer case end	GSRe

Gas heater.- The auxiliary thruster design differs in several respects from the prime thruster design previously described. These changes are intended to alleviate the problems associated with small size engines.

1) Two passes are used for the regenerative preheater in an effort to recover more of the heat lost by conduction through the thermal insulation.

2) The heater coil and its annular passage (the third pass) are truncated in length at the stem end to reduce the flow of heat from the heater to the mounting base and the stem. Convective heat transfer benefits from the high temperature gradients in small engines. The remaining passage length appears to be adequate for initial heating of the gas.

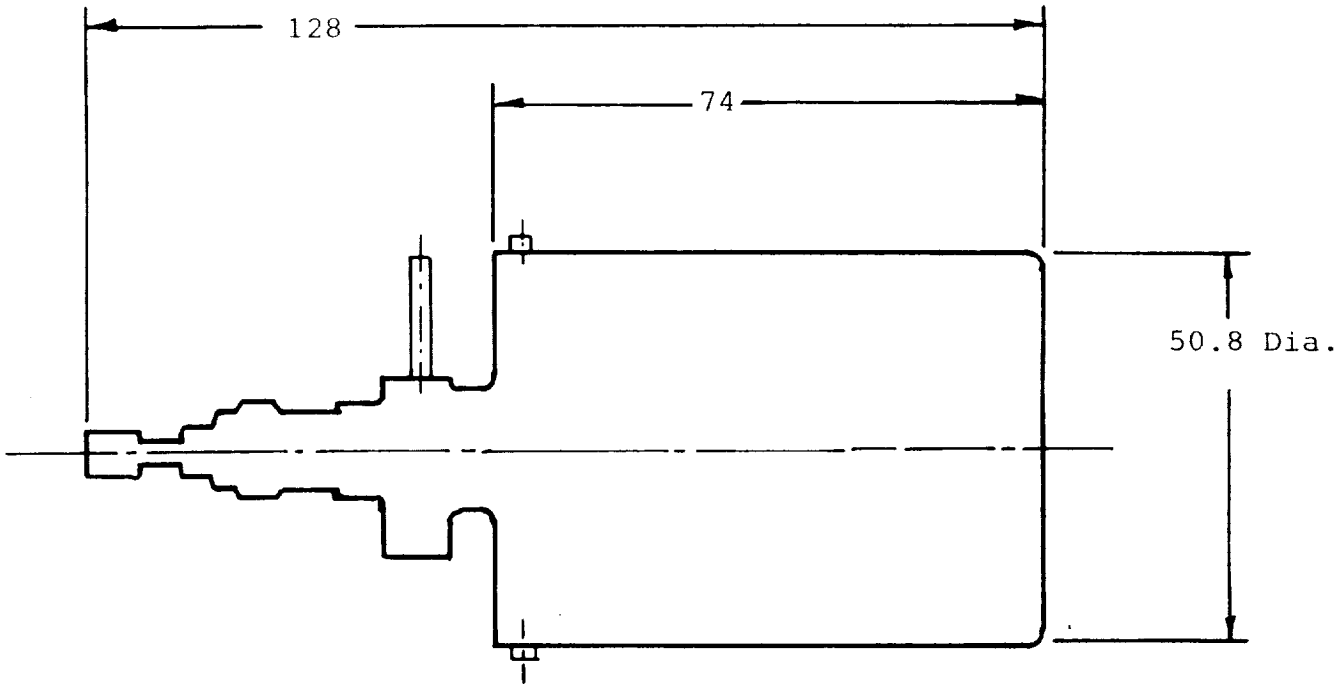

a) Model II (ref. 3)

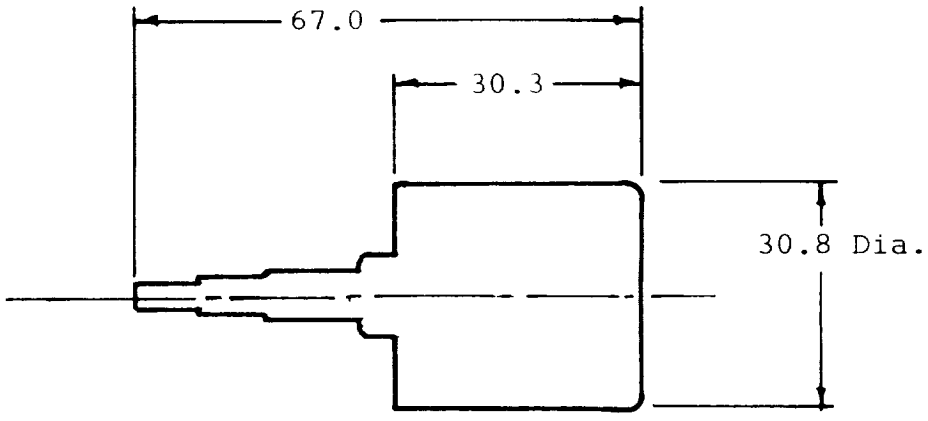

b) Auxiliary thruster of this study

Figure 9.- Comparative profiles of the auxiliary thruster (44.4 mN) of this study with its predecessor, Model II (10 mlb_f) life test unit (ref. 3). Dimensions in mm.

3) The fourth pass is an annular passage enclosing a tubular mesh heater. The mesh is formed by two concentric coils of opposite rotation. The wire intersection points are spot welded to provide adequate rigidity while maintaining high electrical resistance. The heater structure is rigid enough to allow the coil to be free standing without the need for insulating liners on the tube surfaces. This pass can therefore run at the maximum allowable rhenium temperature. It is a highly effective heater. It takes the place of three or four passes of nested tube heaters, and does the job with higher electrical resistance permitting direct operation from a 28 volt power source. The fifth and final pass consists of the center tube which carries electrical current and provides a small additional amount of heating. The action is similar to that of the final pass used in earlier designs. Some heat is lost due to the cooling effect of the nozzle, but the level of loss is kept moderate by designing for reduced heating in this pass.

4) Simple hand calculations were used to select a modified stem design that could be expected to run with a satisfactory temperature in the seal region. the selected design increased the stem length to three centimeters and added radiation fins at the extreme end of the stem. The fins were taken as equivalent to a disk of alumina 5 centimeters in diameter and 0.25 centimeters thick. The presence of the fins increases the thermal loss through the stem, but the loss is held to less than 8 watts by the increased stem length. The net effect of the two changes is to increase the temperature drop in the stem.

5) To further reduce the temperature in the stem, a radiation shield was introduced across the cavity joining the interior surfaces of the stem with the hot hemispherical ending of the concentric tubular stage.

Nozzle.- The nozzle is defined by table IX.

TABLE IX
NOZZLE DESCRIPTION FOR 44.4 mN DESIGN

Configuration	Conical
Half angle, α	18°
Area ratio, (geo.)	178
Throat (geo.), mm	.348±.005

Systems.- The specific characteristics of the heating system are described by figure 8 and table X. The materials of construction are the same as used for the 667 mN thruster.

TABLE X
PHYSICAL DIMENSIONS

a) Coiled heaters

	First stage (1)	Second stage (2)
Heater wire diameter, mm	.254	.203
Number of parallel circuits	3	4*
Coils per circuit (series)	2	1
Circuit wire length, mm	61	148.6
Total heater wire length, mm	365	595.4

*2 clockwise/2counter

b) Concentric tubular heaters

	Domed Pressure Vessel (5)	Tubular Inner (6)
Outer diameter, mm	3.85	1.35
Wall thickness, mm	.15	.125

Results and Discussion of Results

Estimated performance.- Results of the steady state computer analysis of the 44 mN thruster are shown in table XI for both hydrogen and ammonia propellants for a gas stagnation temperature of 2500°K at the nozzle throat in both cases. Temperatures are plotted in figures 10 and 11 and the calculated energy distribution is shown in figure 12. A comparison of these figures with those for the 667 mN thruster show a significant penalty in performance associated with the small engine size. Estimated heater efficiencies have dropped from 96 percent to 88 percent for hydrogen, and from 94 percent to 82 percent for ammonia. As expected, the heat flow radially outward through the insulation is a much larger fraction of the total electrical power in the small engine case, making it necessary to take special care in the design of the regenerative heating passages to recover most of this energy.

The performance of the small thruster is seen to be poorer in another respect. The maximum wall temperature, which occurs on the second heater coil near its downstream end, is 168° to 186° hotter than the stagnation gas temperature attained at the nozzle throat. This compares to a temperature differential of only 50° to 55°K for the prime thruster case. To some extent, the poorer performance is inherent in the small sized engine.

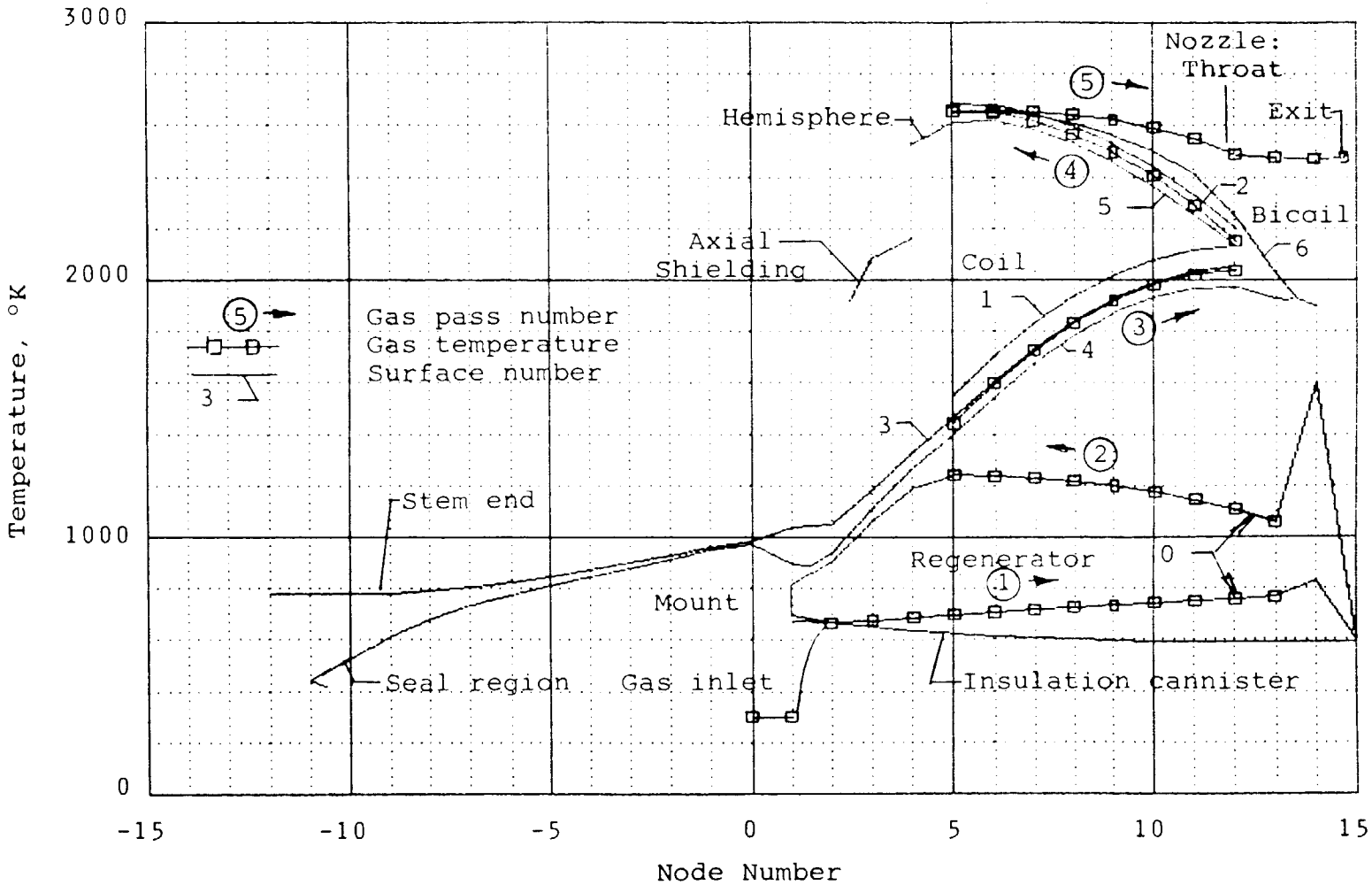

Figure 10.- Temperature distribution from the thermal modeling analysis of the 44.4 mN hybrid concentric tubular resistojet operating on hydrogen.

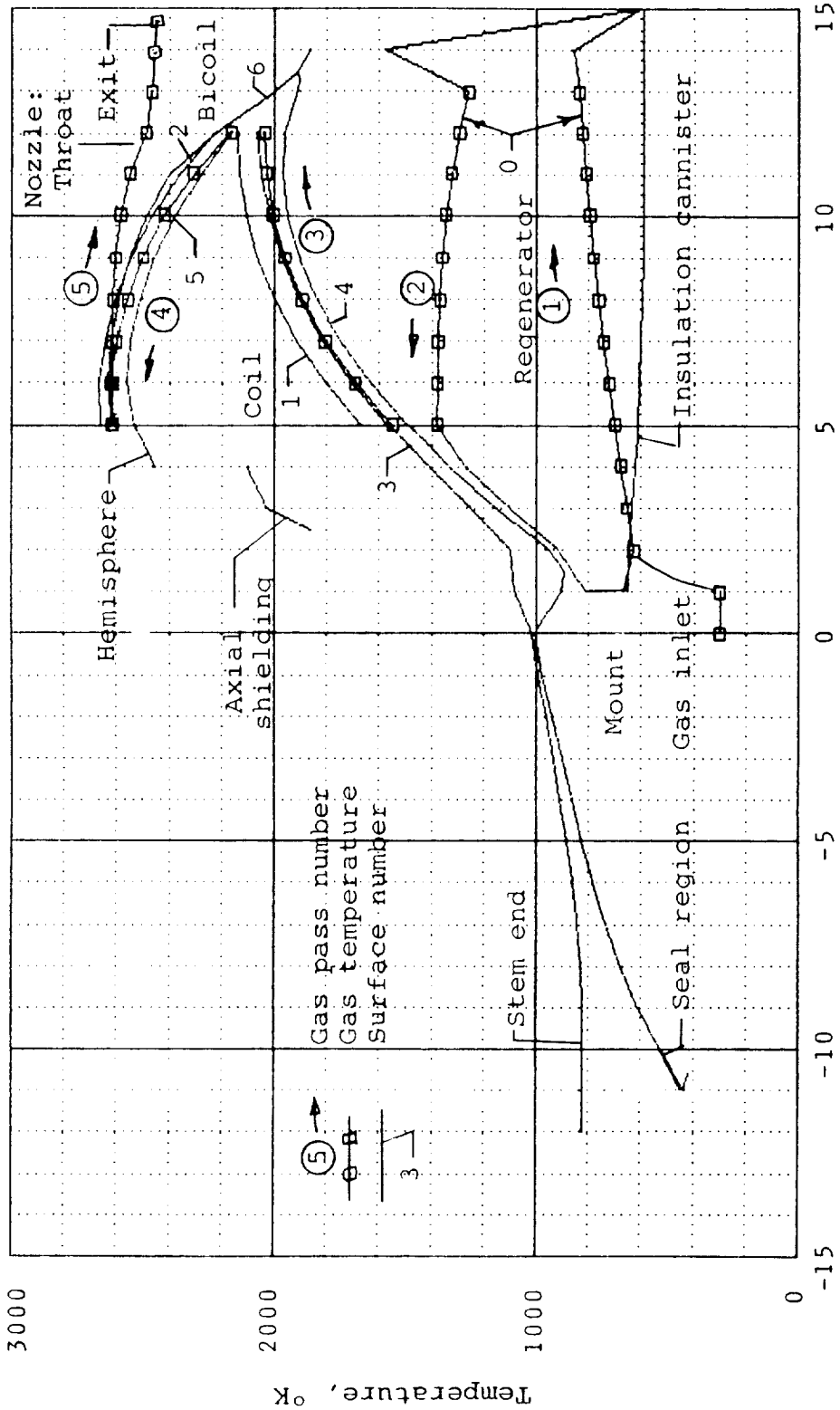

Figure 11.- Temperature distribution from the thermal modeling analysis of the 44.4 mN hybrid concentric tubular resistojet operating on ammonia.

ORIGINAL PAGE IS
OF POOR QUALITY

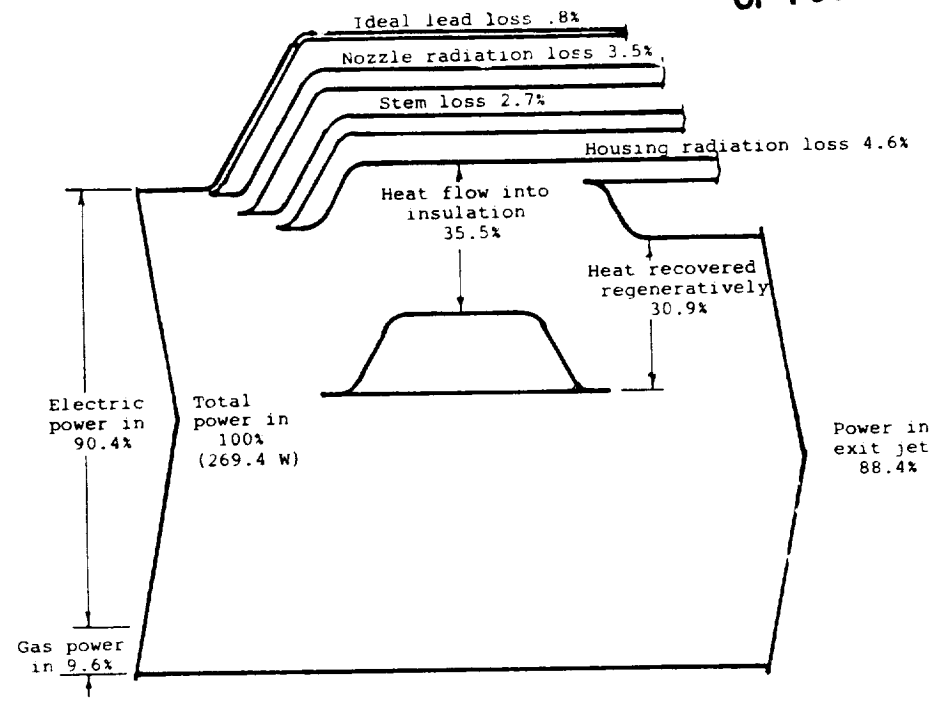

a) Hydrogen

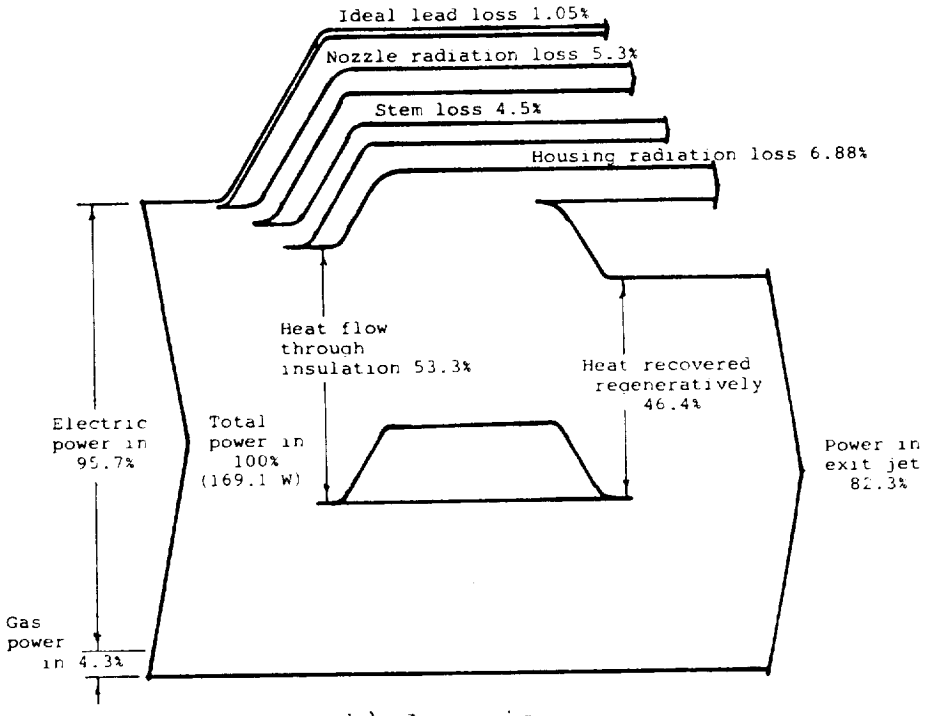

b) Ammonia

Figure 12.- Estimated steady state energy distribution of the 44.4 mN hybrid concentric tubular resistojet at total gas conditions of temperature of 2500°K and pressure of 3.16 atmospheres at the throat.

Larger portions of the heat in the gas are lost by convection to the cool wall near the nozzle; and in turn, the wall is cooled to a greater extent by increased conduction into the housing and by increased convection to the gas in the adjoining passage. However, the latter effect has been accentuated by the use of the second heater coil which heats the gas rapidly resulting in a strong axial temperature gradient. Unfortunately, the cool end of the pass is adjacent to the nozzle and adds to the cooling of the center tube where the flow approaches the nozzle. This suggests that adjustments might be considered in the heating element designs to increase the heating rate near the nozzle. A trade-off between high specific impulse and good efficiency is involved.

Table XI summarizes the projected performance of the 44mN design resulting from this analysis.

TABLE XI
ESTIMATED PERFORMANCE FOR AUXILIARY THRUSTER

Propellant	H_2	NH_3
Thrust, mN	44.4	44.4
Gas temperature, °K	2500	2500
Chamber pressure, atm	3.16	3.16
Specific impulse, sec	757	375
Expellant flow, mg sec^{-1}	5.99	12.10
Electric power, W	243.6	161.9
Total power, W	269.4	169.1
Terminal voltage, V	28	22
Current, A	9.053	7.351
Total power efficiencies		
Overall, η_o	0.597	0.467
Heater, η_H	0.884	0.823
Nozzle, η_N	0.673	0.567

CONCLUDING REMARKS

1. The design technique used to forecast energy and temperature distribution in resistojets using mathematical modeling by small microcomputer was found to rapidly predict results for the designs here.

2. Where compared with earlier experimental tests the model did explain earlier results, resulting in their design correction.

3. The technique of raising appreciably the voltage characteristics of concentric tubular resistojets for better matching the space station power sources by using a hybrid design of a high resistance inlet stage in series was successful. The 28 volt terminal voltage objective can be met for all designs studied here.

4. The exit gas temperature can be made to closely approach maximum wall temperature by use of the modeling technique. The differences ranged from 55°C in the 667 mN design. It is more difficult with the smaller 44.4 mN thruster where the maximum wall temperature required was 186°C over that of the gas at nozzle throat.

5. The study of gas dynamic performance in nozzles by mathematical modeling not undertaken here is recommended for future study.

APPENDIX A

DEFINITION OF PERFORMANCE PARAMETERS

Specific impulse, I_{sp}, seconds

$$I_{sp} = F/\dot{m} \quad \text{(A1)}$$

where F = measured thrust by dynamometer, g
$\dot{m}$ = propellant mass flow, g-sec^{-1}

Electric power to terminals, P_e, watts

$$P_e = E_t \times I_t \quad \text{(A2)}$$

E_t = electric voltage difference between thruster terminals, V
I_t = electric current through terminals

Heater Resistance, R, ohms

$$R = E_t/I_t \quad \text{(A3)}$$

Efficiency - total power overall, η_o

$$\eta_o = F \times I_{sp}/(20.8\ (P_e + P_i)) \quad \text{(A4)}$$

Efficiency - electrical power overall, η_o*

$$\eta_o^* = F \times I_{sp}/(20.8\ P_e) \quad \text{(A5)}$$

Initial power in gas, P_i, watts

$$P_i = \dot{m}\ h\ 4.186 \quad \text{(A6)}$$

h = absolute enthalpy, ideal gas, cal/gm

Power in the jet, P_j, watts

$$P_j = P_e + P_i - P_L \quad \text{(A7)}$$

P_L = heat lost from the thruster prior to the exhaust jet, W

Heater efficiency, η_h

$$\eta_h = P_j/(P_e + P_i) \quad \text{(A8)}$$

Nozzle efficiency, η_n

$$\eta_n = F \times I_{sp}/(20.8\ P_j) \quad \text{(A9)}$$

APPENDIX B

BASIS OF MATHEMATICAL COMPUTATIONAL MODEL
By L. Barker

An IBM P.C. running a compiled BASIC was used to model the resistojet. The compiler uses up to 128 K bytes of memory and then requires a total of about 192K to run. This permitted a node model with about 500 to 600 nodes. Because the total program was too large to be run at once, the BASIC chain command was used to combine two or three subprograms.

The Model

A program has been developed for estimating steady state temperatures and heat flows in a resistojet of the types described. The thruster is represented by a network of nodes joined by heat transmitting elements. Since the thruster utilizes a large number of concentric passages, the node diagram is relatively complex. See figures 14 and 15. There are 224 nodes or junction points connected by nearly 500 heat flow paths. The material identifiers of each element are next assigned, which allows access to the needed material properties subroutine banks as required, e.g., electrical conductivity with temperature, emissivity, etc. The various heat transfer linkages between the various adjacent elements are embodied in the program. Heat transfer procedures for treating nonadjacent nodes and nonasymmetric components are provided on an individual basis. The net heat flow into an element can be determined for its assumed temperature and that of its adjacent elements. Heat flows between nodes are estimated, and wall temperatures are adjusted in successive approximations until a satisfactory heat balance is achieved at all nodes. At the same time, the gas temperature is estimated at each node in the passages; and the electrical currents are adjusted successively to obtain the desired heater coil temperature at the exit to the second pass, and the desired gas stagnation temperature at the nozzle throat. When the net heat flux into each node is zero, the equilibrium temperature throughout the model is found. The method for determining this temperature distribution is next described.

The Method

To solve for a steady-state temperature distribution, the detailed procedure outlined in figure 13 was used. In summary, heat flows between all nodes are calculated using assumed values for temperatures and then are summed for each node. If the sums are not sufficiently small, the temperatures are adjusted and the

calculations repeated. The systematic temperature correction used is a fraction (usually .7) of the following expression:

$$\Delta T_i = \frac{-\sum_{j=1}^{N} q_{i,j}}{\sum_{j=1}^{N} \frac{\partial q_{i,j}}{\partial T_i}}$$

where $q_{i,j}$ = the heat flow into node i from node j.

There is a test for convergence. This section requires that the heat balance error be no more than 0.1 watt for any node and that the heating coil temperature at the down stream end and the gas exit temperature differ from the prescribed values by no more than 0.1°K. If the conditions for convergence are met, the procedure leaves the main loop and jumps to the printout section, and if not, the iterative process continues.

In the next approximation equation for temperatures above, it has been found that the fraction (.7 used here) must be less than unity to stabilize the convergence process. Too high a value can result in increasing errors of alternate sign, while too low a value will reduce the rate of convergence.

When the temperatures have converged, values of heat flows and temperatures are printed out and the temperatures are plotted on a dot matrix printer. For a transient solution, the above approach is used, except instead of the above temperature correction, a similar expression is used which includes mass and specific heat data for each node as well as a maximum allowable time interval. The models used for various heat flow mechanisms follow.

Conduction

The equation used is the Fourier equation:

$$q = -kA \frac{\partial T}{\partial x}$$

In this equation heat flow towards increasing x is positive. In the program heat flow into a node is positive regardless of direction.

For a given qeometry one can assume that q is a constant and that A is a function of x.

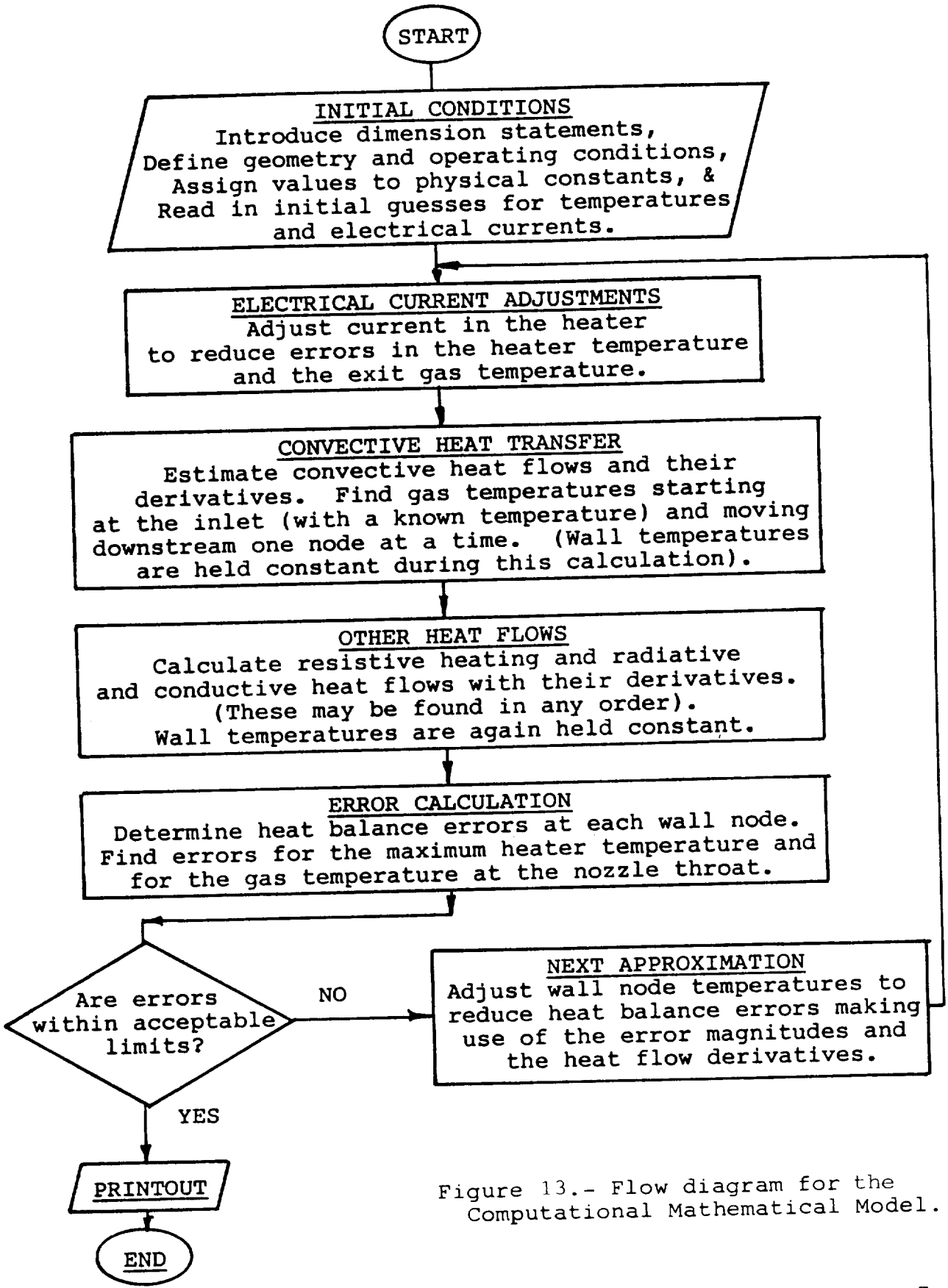

Figure 13.- Flow diagram for the Computational Mathematical Model.

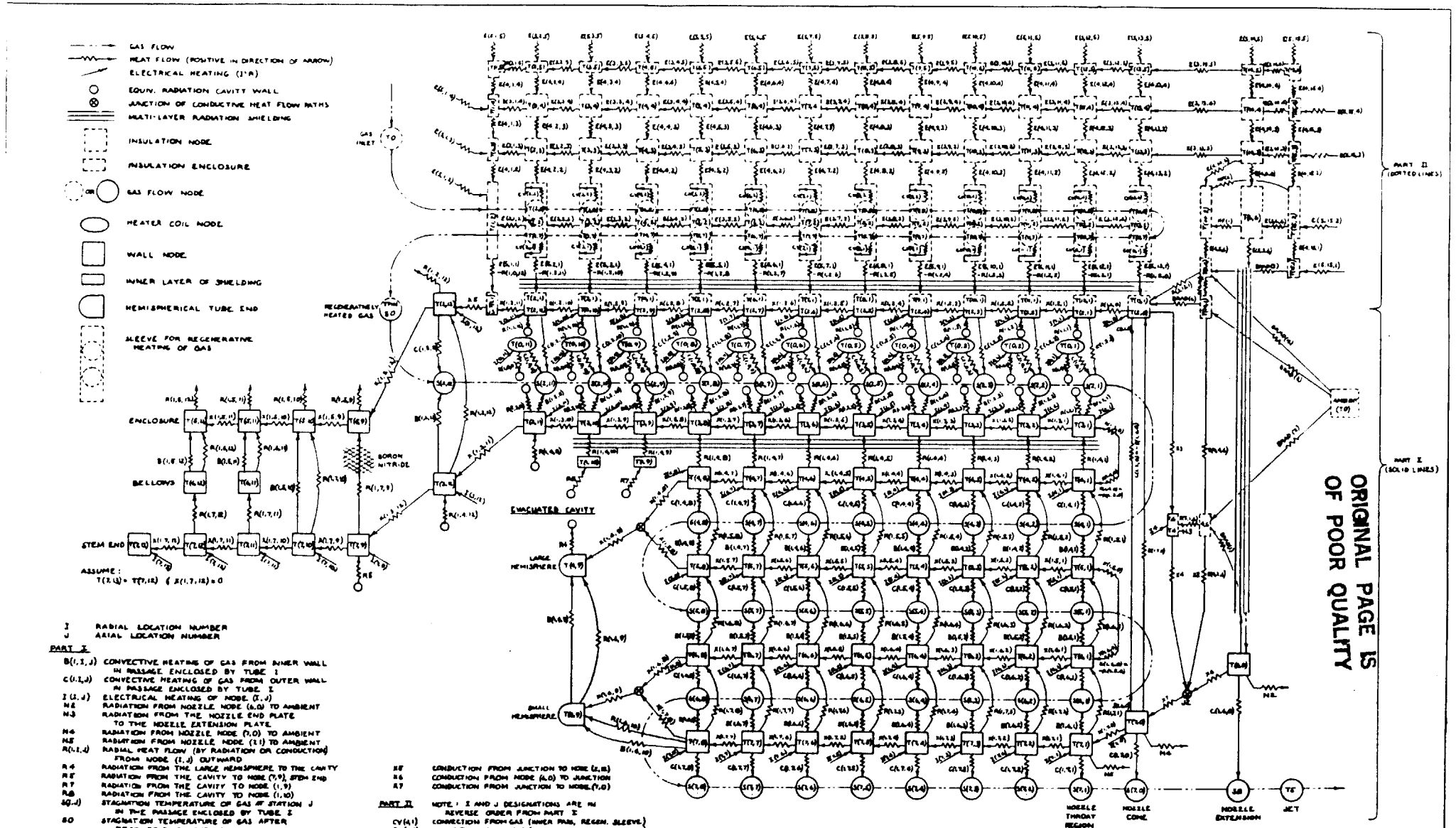

ORIGINAL PAGE IS OF POOR QUALITY

I RADIAL LOCATION NUMBER
J AXIAL LOCATION NUMBER

PART I

B(I,J,J) CONVECTIVE HEATING OF GAS FROM INNER WALL IN PASSAGE ENCLOSED BY TUBE I
C(I,J,J) CONVECTIVE HEATING OF GAS FROM OUTER WALL IN PASSAGE ENCLOSED BY TUBE I
I (I,J) ELECTRICAL HEATING OF NODE (I,J)
R2 RADIATION FROM NOZZLE NODE (6,0) TO AMBIENT
R3 RADIATION FROM THE NOZZLE END PLATE TO THE NOZZLE EXTENSION PLATE
R4 RADIATION FROM NOZZLE NODE (7,0) TO AMBIENT
R5 RADIATION FROM NOZZLE NODE (2,1) TO AMBIENT
R(I,I,J) RADIAL HEAT FLOW (BY RADIATION OR CONDUCTION) FROM NODE (I,J) OUTWARD
R6 RADIATION FROM THE LARGE HEMISPHERE TO THE CAVITY
R7 RADIATION FROM THE CAVITY TO NODE (7,9), STEM END
R8 RADIATION FROM THE CAVITY TO NODE (1,9)
R9 RADIATION FROM THE CAVITY TO NODE (1,10)
ΔQ(J) STAGNATION TEMPERATURE OF GAS AT STATION J IN THE PASSAGE ENCLOSED BY TUBE I
S0 STAGNATION TEMPERATURE OF GAS AFTER REGENERATIVE HEATING
S8 GAS TEMPERATURE IN THE NOZZLE EXTENSION
T(I,J) TEMPERATURE AT STATION (I,J)
T0 AMBIENT TEMPERATURE
T6 NOZZLE END PLATE TEMPERATURE
T8 STAGNATION TEMPERATURE OF GAS LEAVING NOZZLE
R(I,I,J) AXIAL CONDUCTION FROM NODE (I,J) TO NODE (I, J+1)
R1 CONDUCTION FROM THE EXTENSION PLATE TO THE NOZZLE
R3 CONDUCTION FROM NODE (2,0) TO NOZZLE END PLATE
R4 CONDUCTION FROM NOZZLE END PLATE TO NOZZLE
R8 CONDUCTION FROM JUNCTION TO NODE (2,8)
R6 CONDUCTION FROM NODE (6,0) TO JUNCTION
R7 CONDUCTION FROM JUNCTION TO NODE (7,0)

PART II

NOTE: I AND J DESIGNATIONS ARE IN REVERSE ORDER FROM PART I
CV(I,I) CONNECTION FROM GAS (INNER PASS, REGEN. SLEEVE)
CV (I,8) CONNECTION FROM GAS (OUTER PASS, REGEN. SLEEVE)
E(I,J,I) AXIAL CONDUCTION FROM NODE (I+1, I) TO (I,I)
E(I,J,2) RADIAL CONDUCTION FROM NODE (I, I+1) TO NODE (I, I)
E(I, I, 3) RADIATION FROM AMBIENT TO ENCLOSURE SURFACE
T(I, I) TEMPERATURE OF NODE (I, I)
T0 AMBIENT TEMPERATURE
TPIN STAGNATION TEMPERATURE OF GAS AFTER REGENERATIVE HEATING
BRAD (J) RADIATION THROUGH SHIELDING
HP (J) AXIAL CONDUCTION (EXPRESSED IN TWO PARTS)

Figure 14.- Node diagram - heater computational mathematical model - 667 mN prime thruster.

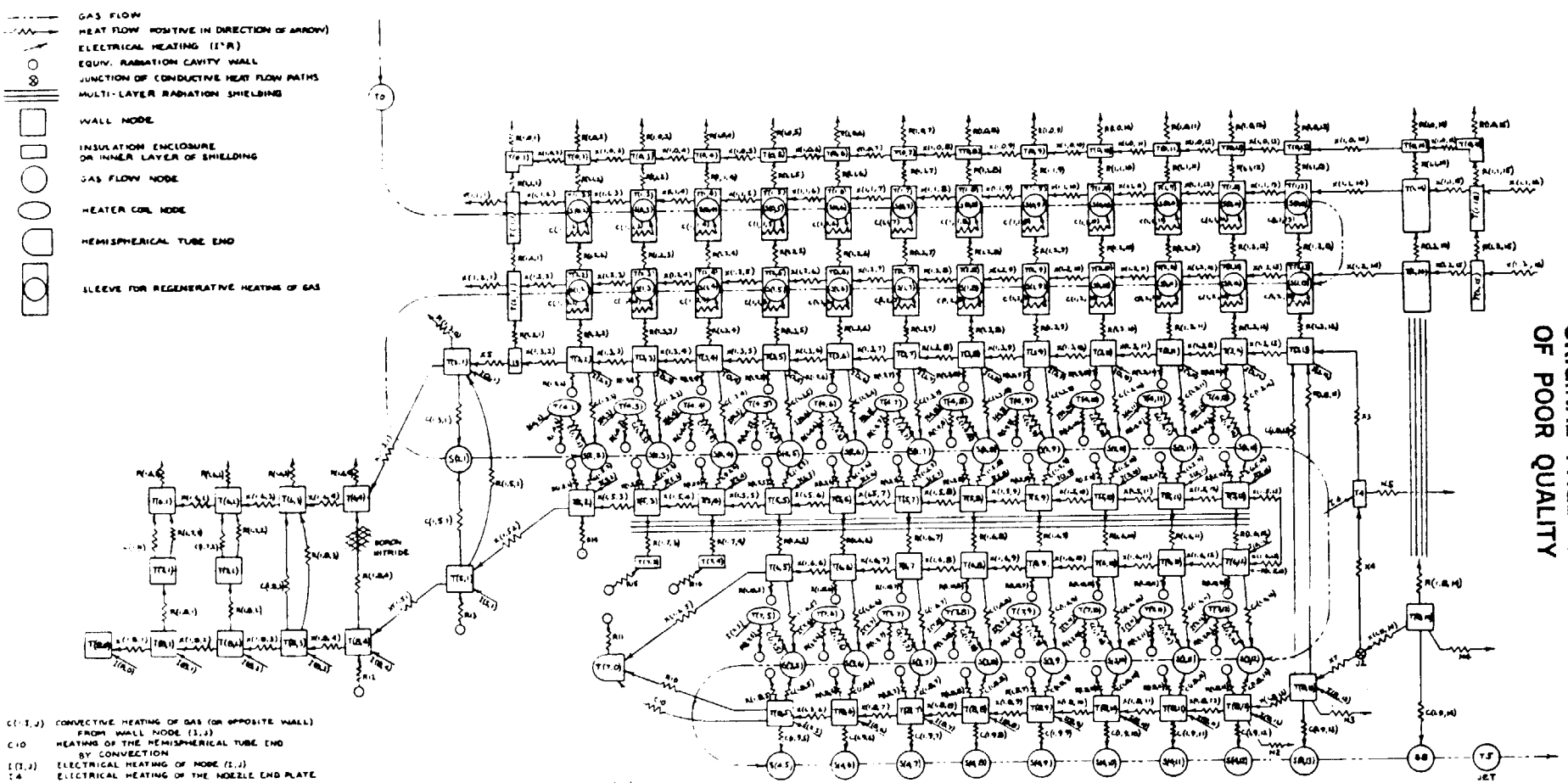

C(I,J) CONVECTIVE HEATING OF GAS (OR OPPOSITE WALL) FROM WALL NODE (I,J)
C10 HEATING OF THE HEMISPHERICAL TUBE END BY CONVECTION
E(I,J) ELECTRICAL HEATING OF NODE (I,J)
E4 ELECTRICAL HEATING OF THE NOZZLE END PLATE
J2 TEMPERATURE OF JUNCTION BETWEEN NODES (8,13) (8,14)
J3 TEMPERATURE OF JUNCTION BETWEEN NODES (3,1) & (3,2)
R1 RADIATION FROM NOZZLE NODE (8,12) TO AMBIENT
R2 (8,13)
R3 (8,14)
R4 RADIATION FROM THE NOZZLE END PLATE THROUGH SHIELDING TO AMBIENT
R(I,I,J) RADIAL HEAT FLOW BY RADIATION OR CONDUCTION
R10 INTERNAL HEATING OF HEMISPHERE BY RADIATION
R11 EXTERNAL COOLING
R12 RADIATION TO NODE (8,4) FROM THE STEM END CAVITY
R13 (5,1)
R14 (6,6)
R15 (7,3)
R16 (7,4)
T(I,J) GAS TEMPERATURE AT NODE (I,J)
T8 GAS STAGNATION TEMPERATURE IN THE NOZZLE EXTENSION NODE

TT(I,J) WALL TEMPERATURE AT NODE (I,J)
TO AMBIENT TEMPERATURE AND INLET GAS TEMPERATURE
T4 NOZZLE END PLATE TEMPERATURE
T5 GAS STAGNATION TEMPERATURE IN THE JET
X(I,I,J) AXIAL HEAT FLOW FROM NODE (I,J) TO NODE (I,J-1) BY RADIATION OR CONDUCTION
X3 CONDUCTION FROM THE NOZZLE END PLATE TO NODE (3,13)
X4 CONDUCTION FROM J2 JUNCTION TO NOZZLE END PLATE
X5 CONDUCTION FROM J3 JUNCTION TO NODE (3,1)

Figure 15.- Node diagram - heater computational mathematical model - 44.4 mN auxiliary thruster.

Or, rearranging terms:

$$\frac{q}{A(x)} = -k(T)\frac{dT}{dx}$$

For axial conduction A(x) = A, a constant.

$$\text{and } q = \frac{A}{(x_2 - x_1)} \int_{T_2}^{T_1} k\,(T)dT$$

For radial conduction A(r) = 2πr dx

$$\text{and } q = \frac{2\pi dx}{\ln\left(\frac{r_o}{r_i}\right)} \int_{T_o}^{T_i} k(T)dT$$

where,

$r_o = r_{outer}$
$r_i = r_{inner}$

For nodes that are neither axial nor radial, a linear area variation is assumed approximately orthogonal to flow path.

Thus, $A(L) = aL$

$$\text{and } q = \frac{a}{\ln\ L_2/L_1} \int_{T_2}^{T_1} k(T)dt$$

To simplify the problem, when adjacent nodes are not of the same material, a heat flow resistance approach is used.

$$\text{In the program, } q_1 = \frac{2(T_2 - T_1)}{(R_1 + R_2)}$$

Where $R_{axial} = dx / (Ak(T))$

$R_{radial} = \ln(r_o/r_i) / (2\pi dx k(T))$

and $R_{axial} = \ln(L_2/L_1) / (ak(T))$

Convection

The equation used for tubes is:

$$q = (ANuk / D_h)\ (T_w - T_g)$$

Where D_h = hydraulic diameter = 4(flow area/flow perimeter)

If the propellant temperature is not known, then the energy received by it is equated to its heat capacity to obtain

$$T_g = T_w + (T_{go} - T_w)e^{(-hA/\dot{m}C_p)}$$

where T_{go} = initial gas temperature.

and then

$$q_w = (T_{go} - T_g)\ \dot{m}Cp$$

The approach for annual passages is described in Kays (Ref. 29).

$$\text{Where } q_i = \frac{A_i}{D_h(1-\theta_i\theta_o)}\ (K_iNu_i\ (T_i-T_m)+\theta_iK_oNu_{oo}(T_o-T_m))$$

$$q_o = \frac{A_o}{D_h(1-\theta_i\theta_o)}\ (\theta_ok_iNu_i\ (T_i-T_m) + k_oNu_{oo}(T_oT_m))$$

In the nozzle high velocity region, the approach used is described in Eckert and Drake. The equation used is:

$$q = (ANuk / D_h)\ (T_w - T_{gw})$$

where k and Nu are determined for the reference temperature

$$T^* = T_g + .5(T_w - T_g) + .22(T_{gw}-T_g)$$

$$\text{where } T_o = T_g\ (1 + \frac{\gamma-1}{2} M_g^2) = \text{stagnation temperature}$$

$$T_{gw} = T_g\ (1+r \frac{\gamma-1}{2} M_g^2) = \text{adiabatic wall temperature}$$

and the recovery factor $r = Pr^{1/2}$ for laminar flow and $r = Pr^{1/3}$ for turbulent flow. M_g = the mach number input to the program as a constant for each node in the nozzle which is calculated as a function of gamma (γ) and the ratio of cross-sectional area to throat area.

Radiation

Given two surfaces, the equation used is

$$q_1 = \frac{A_1 (e_{b2} - e_{b1})}{\frac{1}{\varepsilon_1} + \left[\frac{1}{F_{12}} - 1\right] + \frac{A_1}{A_2}\left[\frac{1}{\varepsilon_2} - 1\right]}$$

where $e_{b2} = \sigma T_2^4$

Usually $F_{12} = 1$ and this equation reduces to Christianson's equation. For radiation to ambient $A_2 \rightarrow \infty$ and the equation becomes

$$q_1 = A_1 \varepsilon_1 (e_{b2} - e_{b1}) \qquad \text{where } e_{b2} = \sigma T^4_{amb}$$

For more than two surfaces simultaneous equations are used to solve for the heat transfer.

For each node, adapting the terminology of Eckert and Drake (Ref. 34).

$Q = q/A$ heat transfer per area per time

$e_b = \sigma T_4$ the emissive power, net radiation per area per time

H = net heat flux arriving at node

B = net heat flux leaving the node

$\varepsilon_a = (B/e_b)$ the apparent emissivity

$\varepsilon H =$ the absorbed part of H

Then, $Qi = \varepsilon_i H_i - \varepsilon_i e_{bi}$

where $$H_i = \frac{1}{A_i} \sum_{k=1}^{N} (A_k F_{ki} \varepsilon_{ak} e_{bk})$$

or $$H_i = \sum_{k=1}^{N} (F_{ik} \varepsilon_{ak} e_{bk})$$

Thus, for each node i

$$Q_i = -\varepsilon_i e_{bi} + \varepsilon_i \sum_{k=1}^{N} (F_{ik} \varepsilon_{ak} e_{bk})$$

Also,

$B_i = H_i - Q_i$. From this, one can derive

$$\varepsilon_{ai} = \varepsilon_i = \frac{(1 - \varepsilon_i)}{e_{bi}} \sum_{k=1}^{N} (F_{ik}\ \varepsilon_{ak}\ e_{bk})$$

This set of equations can be solved for the ε_a's and by substituting into the equation q_i can be found. Or, when $\varepsilon_i <> 1$, the equation can be reduced to

$$Q_i = \frac{\varepsilon_i}{1-\varepsilon_i} e_{bi} (e_{ai} - 1)$$

REFERENCES

1. Pisciotta, A.,Jr.; and Eusanio, E.N.: Definition of a Resistojet Control System for the Manned Orbital Research Laboratory. Final Report, Vol. 1, Summary NASA CR-66600 (DAC-58130) May 1968.

2. Greco, R.V.; and Bliss, J.R.: Resistojet System Studies Directed to the Space Station/Space Base. Vol.1 Station/Base Biowaste Resistojet System Design. NASA CR-111879. April 1971.

3. Page, R.J.; and Short, R.A.: Definition of a Resistojet Control System for the Manned Orbital Research Laboratory. Final Report, Vol. V, Resistojet Design and Development. NASA CR-66604 (PAC 58134), May 1968 and Addendum to Vol. V. 720 Hour resistojet Life Test. NASA CR-66604A, Sept. 1968.

4. Page, R.J.; and Short, R.A.: Ten Millipound Resistojet Performance. Journal of Spacecraft and Rockets, Vol. 5, No. 6, July 1968, pp. 857-858.

5. Yoshida, R.Y.; Halbach, C.R.; Page, R.J.; Short, R.A.; and Hill, C.S.: Resistojet Thruster Life Tests and High Vacuum Performance. NASA CR-66970 (TMC S-974), 1970.

6. Page, R.J.; Halbach, C.R.; and Short, R.A.: 3 kW Concentric Tubular Resistojet Performance. Journal Spacecraft and Rockets, Vol. 3, No.11, November 1966, pp. 1669-1674.

7. Page, R.J.; and Short, R.A.: The Design of a Three Kilowatt Hydrogen Thruster. Final Report for Ministry of Technology (Britain). Advanced Rocket Technology, Irvine, CA 1970.

8. Donovan, J.A.; Lord, W.T.; and Sherwood, P.J.: Fabrication and Preliminary Testing of a 3kW Hydrogen Resistojet. Presented at AIAA 9th Electric Propulsion Conference (Bethesda, MD), April 1972.

9. Donovan, J.A.; and Lord, W.T.: Performance Testing of a 3kW Hydrogen Resistojet. Rocket Propulsion Establishment, Westcott, Aylesbury, Bucks. (England).

10. Page, R.J.; Stoner, W.A.; and Barker, L.: A Design Study of Hydrazine and Biowaste Resistojets. NASA CR- 179510, Sept. 1986.

11. Pisciotta, A.,Jr; and Eusanio, E.N.: Definition of a Resistojet Control system for the Manned Orbital Research Laboratory. Final Report, Vol. 2, Resistojet control System Analysis. NASA CR-66600 (DAC)-58130) May 1968. Appendix - Optimized Resistojet Performance Predictions-Nozzle Analysis.

12. Barr, F.A.; and Page, R.J.: Slip Casting and Extruding Shapes of Rhenium with Metal Oxide additive. Final Report Vol. II Development of Grain Stabilized Rhenium Parts for Resistojets. NASA CR-180851, November 1987.

NASA
National Aeronautics and Space Administration

Report Documentation Page

1. Report No.	2. Government Accession No.	3. Recipient's Catalog No.
NASA CR-182176		

4. Title and Subtitle	5. Report Date
Preliminary Design Study of Hydrogen and Ammonia Resistojets for Prime and Auxiliary Thrusters	October 1988
	6. Performing Organization Code: None

7. Author(s)	8. Performing Organization Report No.
Russell J. Page, Willis A. Stoner, and Larry Barker	
	10. Work Unit No.: 506-55-22

9. Performing Organization Name and Address	11. Contract or Grant No.
R. J. Page Company Santa Ana, California	NAS3-23337
	13. Type of Report and Period Covered: Contractor Report Final

12. Sponsoring Agency Name and Address	14. Sponsoring Agency Code
National Aeronautics and Space Administration Lewis Research Center Cleveland, Ohio 44135-3191	

15. Supplementary Notes

Project Manager, James S. Sovey, Space Propulsion Technology Division, NASA Lewis Research Center

16. Abstract

Designs of high performance resistojets for primary and auxiliary propulsion are described. Thruster power for the primary propulsion application was in the 2 to 3 kW range while auxiliary propulsion power per thruster was 0.15 to 0.25 kW. Propellants considered were hydrogen and ammonia. The report describes design techniques that are used to forecast the temperature and energy flux distributions using mathematical modeling by a personal microcomputer. BASIC language is used throughout to give the designer rapid interaction and control. Both designs integrate compact first stage coils with concentric tubular heaters. The hybrid heater design allows better thruster power matching with the spacecraft power bus. Projected specific impulse levels were 760 to 830s for hydrogen and 380 to 410s for ammonia.

17. Key Words (Suggested by Author(s))	18. Distribution Statement
Resistojet; Rhenium; Space Propulsion; Electric Propulsion	Unclassified - Unlimited Subject Category 20

19. Security Classif. (of this report)	20. Security Classif. (of this page)	21. No of pages	22. Price*
Unclassified	Unclassified	48	A03

NASA FORM 1626 OCT 86

*For sale by the National Technical Information Service, Springfield, Virginia 22161